Long-Term Reliability Study of Photovoltaic (PV) System Installation on Islands

APEC Energy Working Group

July 2017

Acknowledgments

Contents

Figures

Tables

Executive Summary:

A list of major failure mechanisms for crystalline silicon modules at Penghu islands is given in Table1and failure rates as shown in Figure 1.

Table 1. Failure Modes for Crystalline Silicon Modules at Penghu islands

Failure Modes	
Bypass Diode Failures	10%
Broken Cells	10%
Ground Faults	4%
Corrosion	69%
non-performance	7%

Figure 1. Failure rates after IEC 61215 Qualification Testing at Penghu islands
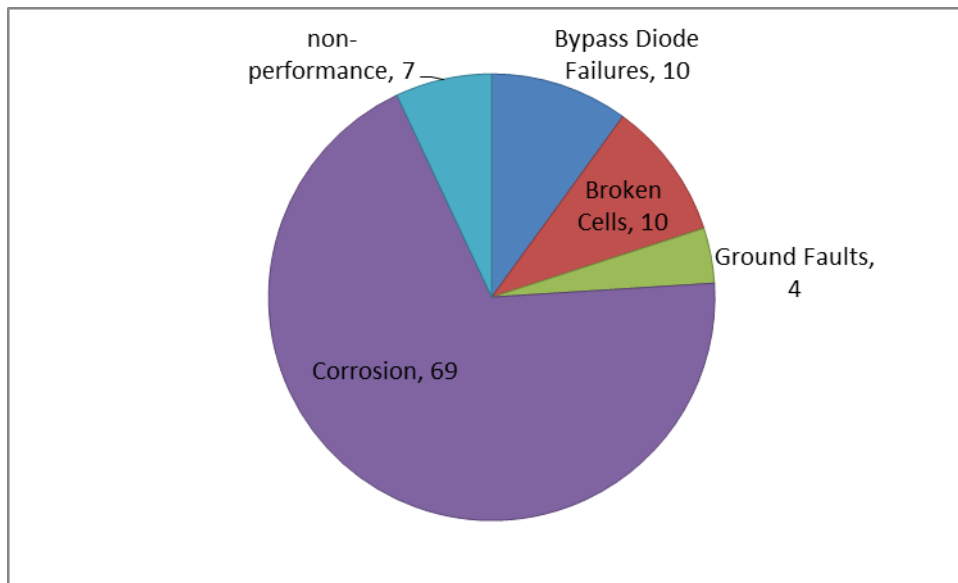
Solutions for manufacturers, system designers, and installers

1. Corrosion:

In the solar industry, most of the racking system components (including the solar module frames) are either mill finish aluminum (aluminum alloy) or anodized aluminum (increased corrosion resistance). There are some bolts and nuts that are stainless steel, bronze or brass. The installer has to be careful in choosing the right material. We usually suggest using anodized components to prevent corrosion for the PV systems that are near ocean.

- Use one material to fabricate electrically isolated systems or components where practical.
- If mixed metal systems are used, select combinations of metals as close together as possible in the galvanic series, or select metals that are galvanically compatible.
- Avoid the unfavorable area effect of a small anode and large cathode. Small parts or critical components such as fasteners should be the more noble metal.
- Insulate dissimilar metals wherever practical [for example, by using a gasket]. It is important to insulate completely if possible.
- Apply coatings with caution. Keep the coatings in good repair, particularly the one on the anodic member.
- Add inhibitors, if possible, to decrease the aggressiveness of the environment.
- Avoid threaded joints for materials far apart in the series.
- Design for the use of readily replaceable anodic parts or make them thicker for longer life.
- Install a third metal that is anodic to both metals in the galvanic contact

Table 2 is list of best practices for corrosion prevention.

Table 2. Galvanic Series (Corrosion Index)

Least Noble (Anodic) - Most Active
Magnesium
Zinc
Aluminium alloys
Low alloy steel
Cast iron
Lead
Alumninum bronze, brass
Copper
Bronze (manganese, silicon)
Nickel, Silver
Stainless steel 302, 304, 316, Alloy 20
Titanium
Gold, Platinum
Graphite
Most noble (cathodic)

Sources:

1. https://www.civicsolar.com/support/installer/articles/galvanic-corrosion-and-protection-solar-pv-installations
2. Guide to Corrosion Prevention and Control, AMMTIAC.
3. Galvanic Corrosion Considerations for PV Arrays, Erika Weliczko, Solar Pro Magazine June/July 2011.
4. Galvanic Corrosion, Wikipedia.
5. Galvanic Table or Galvanic Series of Metals in Seawater, corrosionist.com.
6. Handbook of Corrosion Engineering, Pierre R. Roberge.

2. broken cells , bypass diode failures and other failures

Some tools help to inspect broken cells, like outdoor EL to test in situ. A sequence stress test to evaluate the sensitivity of a particular module type to cell breakage – maybe Cyclic (dynamic) mechanical loading followed by TC & HF.

The next important step was the identification of accelerated stress tests that would duplicate these failure modes in a reasonable short amount of time to solution these

failures. The list in Table 3 was utilized to establish the initial qualification tests that grew into IEC 61215.

Table 3. Accelerated Stress Tests for PV

Thermal Cycles	Broken interconnect
	Broken cells
	Electrical bond failure
	Junction box adhesion
	Module open circuit – potential for arcing
Damp Heat	Corrosion
	Delamination
	Encapsulant loss of adhesion & elasticity
	Junction box adhesion
	Electrochemical corrosion of TCO
	Inadequate edge deletion
Humidity Freeze	Delamination
	Junction box adhesion
	Inadequate edge deletion
UV Test	Delamination
	Encapsulant loss of adhesion & elasticity
	Encapsulant & backsheet discoloration
	Ground fault due to backsheet degradation
	Degradation of Optics
Static Mechanical Load(Simulation of wind and snow load)	Structural failures
	Broken glass
	Broken interconnect ribbons
	Broken Cells
	Electrical bond failures
Dynamic Mechanical Load	Broken glass
	Broken interconnect ribbons
	Broken Cells
	Electrical bond failures
Hot spot test	Hot spots
	Shunts in cells or at scribe lines

	Inadequate by-pass diode protection
Hail Test	Broken glass
	Broken cells
	Broken Optics
By-pass Diode Thermal Test	By-pass diode failures
	Overheating of diode causing degradation of encapsulant, backsheet or junction box
Salt Spray	Corrosion due to salt water & salt mist
	Corrosion due to salt used for snow and ice removal

Sources:

1. IEC 61215-1:2016, Terrestrial photovoltaic (PV) modules – Design qualification and type approval –Part 1: Test requirements.
2. IEC 61215-2:2016, Terrestrial photovoltaic (PV) modules – Design qualification and type approval –Part 2: Test procedures.
3. John H. Wohlgemuth and Sarah Kurtz, Reliability Testing Beyond Qualification as a Key Component in Photovoltaic's Progress Toward Grid Parity.

1 Failure Mode Analysis of Aged PV Module

1.1 The Geographical Environment and Natural Conditions of Penghu Islands
   Geography and Geographic Location:

Figure 1.1.1 Penghu bridge

(source: http://www.penghu-
nsa.gov.tw/English/ShopDetailEn.aspx?Cond=bcd530cb-32e6-4b7a-ae23-
9c30a6877edd)

Figure 1.1.2 Overview of Penghu Islands

(source: http://penghusunrisebnb.theweb.tw/kitesurfing/windsurfing_spots.html)

Figure 1.1.3 Native Architecture of Penghu Islands

Like pearls scattering in the East Sea, the Penghu archipelago is located in the southwest of the Strait. The location is between Chiayi County and Kinmen County, facing Chinese Taipei in the east, and Fujian Province in the west, linking

Matsu archipelago, Dachen Island and Zhoushan archipelago in the north, and Dongsha Islands and Nansha Islands in the south. Located midway betweenChinese Taipei and China in theStrait, Penghu possesses an important geographical position.

The Penghu archipelago consists of nearly one hundred islands. The land area totals about 127 square kilometers. Magong Island (including Magong City and Huxi) is the largest island in the archipelago, followed by Xiyu and Baisha. Only 20 islands are inhabited. The archipelago is located between 23°47' to 23°9' North in latitude and 119°18' to 119°42' East in longitude.

The Penghu archipelago, lying in the middle of theStrait, is the only island whose coastlines are formed of basalt magma. It is the hometown of sea and wind as well as basalt.

Penghu Islands is the only island county of Chinese Taipei. During low tide, more than one hundred isles appear. Therefore, the number of total isles varied. During rising tide, there are, generally speaking, 90 isles scattered between latitude 23°12'to 23° 47' North and longitude 119°19' to 119°43' East. The utmost east isle is Zhamu Isle, the utmost west isle is Hua Isle, the utmost south isle is Cimei Isle, and the utmost north isle is Dogiao Isle. The utmost west isle is also the utmost west boundary ofChinese Taipei. Another unusual thing about Penghu is that the tropic of cancer goes through Hoojing Isle, one of the 90 isles.

Figure 1.1.4 The bird reservation area at Cat Island

(source: http://yacht.ph-sdk.com.tw/index.asp?s=tour&p=8)

Measurement of the Area

Penghu archipelago is scattered across the ocean, extending around 60 km north to south, and 40 km west to east. The combined area of the 90 isles is around 127.9636 square kilometers. Of the 19 isles that are inhabited, the total area is 124.9392 square kilometers. Of the 71 isles that are uninhabited, the total area is 3.0244 square kilometers. The biggest isle is Magong Isle, and the other 4 big isles in order by size are Yuweng Isle, Baisha Isle, Cimei Isle and Wang-an Isle.

Figure 1.1.5 Pescadors lighthouse

(source: Wikipedia)

Landforms

The coastline of Penghu is crooked and lasts for 448,974 m long. Other than the common cape bays, we can also see wave-erosion platform, wave-erosion cliff, wave-erosion cavity, sandy coast and rocky coast landforms along the coast area.

Figure 1.1.6 Wave-erosion cliff

The lay of the isles is mostly gentle and almost every isle is surrounded by cliffs. The top is flat with no obvious ups and downs to be felt. It is a typical square mountain terrain. The main reason for this land formation is that the submarine volcanos erupted basalt flow. This flow came out with layers of water-made rock formations of marine fossil. After numerous slow activities under the sea, a flat

land form. Following a number of sea level changes, the landform emerged is exposed in the air, and eroded into what it looks like today. It is the most obvious feature of Penghu.

The lay of the land slopes gently from south to north with the highest point at 70 m on Damao Isle. Going north by order are 64 m on Cimei Isle, 54 m on Wang-an, 56 m on Magong, 24 m on Baisha, 18 m on Jibei and 14 m on Mudou, finally reaching Da-yao and Er-yao, which are reef formations.

Geology Soil

Figure 1.1.7 The basalt structure of Penghu Islands

The soil formation in Penghu is mainly influenced by climate and geological distribution. Soil distribution and categorization is quite simple, too. Its soil is mostly formed by basalt and coral reef. Different coasts are influenced by different tides and sea winds, and therefore form different kinds of soil. Soil can be divided them into two categories: the ancient geological soil, and the basalt soil. The former is mainly formed by feldspar containing sodium; and secondarily contains mica, amphibole, and augite; it is neutral to acidic. The latter is mainly formed by basalt, calcium feldspar and augite; it is neutral to alkaline.

Temperature

Penghu is located at the edge of the Asian continent and its climate is deeply influenced by regional climate. Penghu is roughly located on the Tropic of Cancer. Its annual average temperature is 23°C, with low at 16.2°C in February and high at 28.3°C in July. Surrounded by the ocean, the temperature in Penghu should be

moderate. However, because of the lack of vegetation on the ground, Penghu is heated by the sunshine in the summer and becomes hot despite the south wind. In the winter, with the strong northeast trades blowing, people feel colder than it really is.

Rainfall

Due to the flat terrain and lack of high mountains, orographic rain formation is impossible. The average annual rainfall is only 1000 mm. With factors such as wind velocity and sunshine, the annual evaporation can reach 1600 mm.

The difference between dry season and rainy season is obvious. October to March of the following year is the dry season, and the amount of rainfall is around 200 mm; April to September is the rainy season, during when the amount of rainfall is around 800 mm. It rains about 95 days a year.

The rain in Penghu is neutral (June 1, 1997, pH 7.69 according to the measurement taken from monitoring station of the government). This is because this area has less air pollution and less chemical compounds that cause acid rain. In addition, when seawater evaporates and forms salt that suspends in the air, the salt is eventually absorbed by the rainfall, which might even make the rain alkaline.

Monsoon

The strong monsoon is a natural phenomenon in Penghu. Penghu is located in the monsoon area and when the northeast monsoon goes throughStrait, which shaped like a tunnel, during autumn and winter, its blast strengthens and often bathes Penghu in its chilly wind. Under this monsoon system, Penghu is enveloped with the winter wind from high latitude regions, mostly from the northeast. Because of the lack of landform as protection, the wind speed in Penghu is quite fast in the winter, maintaining at 6 m/sec or above (which equals level 4 on the Beaufort scale) from October to next January. However, when the continental cold air mass moves south, wind speed could reach level 8 and sometimes 12. The wind velocity changes greatly in Penghu depending on the season. Wind velocity is over 10 m/s in the winter 56% of the time, while in the summer only 7.5%. On the other hand, wind velocity is under 5 m/s only 15% of the time in winter and 54% in the

summer. This reduces activities and the number of tourists in Penghu during the winter, which is also the dull season of Penghu.

Daily change of the wind direction and wind velocity is not obvious. In other areas such asChinese Taipei or neighboring ocean areas, where land winds and sea winds circulate. In the summer, the wind blows from ocean to land during the day, and in the evenings, it blows from land to the ocean. Because Penghu is surrounded by the ocean with small land mass, there is not enough land mass to generate the circadian change in wind direction. Thus, in all winter, the northeasterly wind blows and in all summer, the southwest wind blows.

Ocean

Penghu is surrounded by the ocean with clear water and both the North Shallow Fishing ground in the north and the South Shallow Fishing ground in the south. Also with the branch of the Japan current (the Kuroshio) passing by, it has been a great natural fishing ground since long ago. The main ocean currents are:

- The China coast cold current: this coast cold current influences mostly the west side ocean area of Penghu. It originates from north of the Yellow Sea and flows along the east coast of China toward the south. With a large amount of water pouring in, this current is quite strong especially in the summer with rainfall, and contains little salt. In the winter, this current is strengthened by the northeastern wind and the water temperature is lower than the Japan Current. In the summer, the southwestern wind makes it weaker and the water temperature is similar to the Japan Current. In the winter, fish swims south along with this current and gather up at the west side of Penghu.

- The branch of the Japan Current: the main stream of the Japan Current flows north along the east coast ofChinese Taipei with its branch flowing pass the Bashi Channel and entering the South China Sea to form a counter clockwise current; the other part of the branch turns to flow along the west coast ofChinese Taipei towards north to reach the Penghu area, and then flows further to meet the Japan Current. Stopped by the northeastern wind, this current mostly flows to the South China Sea and only a little part of it flows into the Penghu ocean area. With the summer southwest wind strengthening this current, it mostly flows into the Strait and both the water temperature and the salt content are higher than the other two ocean currents. Therefore, it can bring fishes from tropical Pacific Ocean and the Indian Ocean in the

summer.

- The South China Sea Monsoon Current: in the winter, one branch of the Japan Current and the China coast cold flow go together into the Penghu area and form a counter clockwise current which makes the South China Sea monsoon current influences nothing in this area. In the summer, with strong southwest monsoon blowing, this current flows into theStrait and turn towards northeast. Therefore, this current possesses rich rainfall and river water with it. Generally speaking, in July, the Penghu area is influenced more by the branch of the Japan Current and the South China Sea Monsoon Current. With various cold and warm currents meeting here, a large number of plankton is produced, providing rich foods for great amount of fishes.

Morning and evening tides

There is a tide called "half-day tide" in Penghu. There are two high and low tides every day. Along the coast of both sides of the waterway, the tides flow toward north at high tides and toward south at low tides. Tides have great influence on Penghu. For example, the number of isles. The intertidal zone forms an important working field for the people in Penghu. This zone is also a great place for visitors and tourists to relax.

Waves

According to the Central Weather Bureau, from July 1981 to June 1988, during October to March of the following year, with the winter northeast trades blowing, the waves could be 1.7 m high and 52% of the waves are higher than 1.5 m. During April to September, with the summer southwest monsoon blowing, the waves can be 0.8 m in height and the percentage for waves lower than 1 m is 72%. Sometimes, when the wind and the waves are too strong, transportation on the sea might be interrupted.

1.2 Narrative information of the 16 year-old photovoltaic module/system

The photovoltaic (PV) system was installed on the third floor of the Construction Bureau of Penghu County Government in June 1999. The total area of the solar array is 23.32 square meter. The system can be grid-connected or off-grid connected, which offers 1.5 kilowatt AC (alternating current) electric power during day time. DC combiner box was installed at the array tripod corner. AC power panel, inverter, monitoring system, transformer, and watt hour meter were installed on the first floor wall of the Civil Engineering Department.

The PV system uses polycrystalline silicon solar modules. The open-circuit voltage, operating voltage, short circuit current, and operating current are 24.9 V, 19.5 V, 7.4 A, and 6.92 A under 1000 W/m^2 solar irradiation and 25°C, respectively. Each module's rated output power is 135 Watt (length: 1.12 m, width: 0.971 m, area:1.0875 m^2). The 22 modules are divided into two group according their differences and similarities. Eleven modules with similar electric current output is in series connection.

The rated operating voltage of the PV system is about 214 V. The DC input voltage of the system is about 273.9 V.

The power conversion controller (abbreviated to "controller" in the following sentence) is made by Kyocera, Japan. The capacity of the controller is 3 kilowatt. The minimum and maximum DC input voltage for operation is 116 V and 350 V, respectively. The AC output voltage of the controller is 101 V and 202 V. The phase of the controller is a three-wire single phase system with 60 Hz frequency. The conversion efficiency of the controller is about 95%. The controller also has coupled power grid protection.

The Monitoring System of the PV System

Several sets of transducers were set up to understand the conversion efficiency of the inverter, changing DC current into AC current, and PV modules, changing solar power into DC current. The transducers convert the data, such as module temperature and the analog voltage/current coming from solar irradiation, from analog to digital signal. The digital signal goes through internal RS-485 interface and data collector, which fixed time scan of the mentioned data. The data will be collected and stored in a named format and then pass to PC (personal computer). After PV processes the data, such as DC power, AC power, solar irradiation, and module temperature, etc, the data will become understandable data, such as the amount of sunlight, module temperature trend, daily DC current output, etc. The data will be finished by the monitoring system. In other words, the monitoring system should communicate/collect/process with data collector. Figure 1.2.1 shows the architecture of the monitoring system.
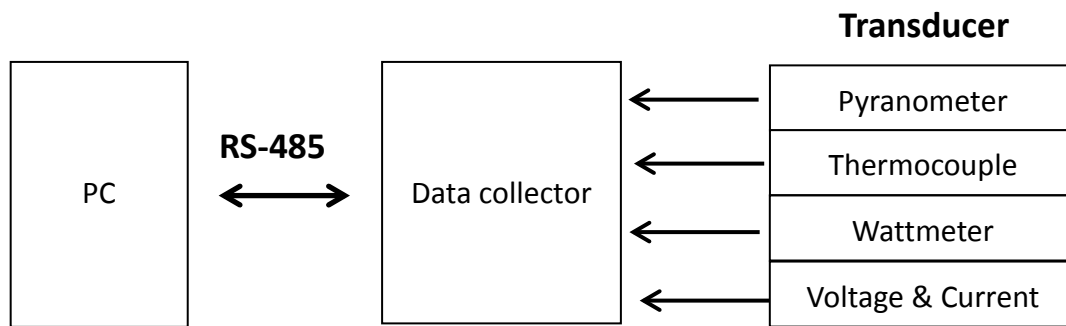
Figure 1.2.1: architecture of the monitoring system

Specifications of the measurement tools of the PV system

1. Shunts
    Maximum operating voltage   1000 V
    Measurement range   20A/50 mv

2. Current transformer
    Maximum operating voltage   600 V
    Measurement range   30 A/5 A

3. Mechanical watt hour meter
    Maximum operating voltage   600 V
    Maximum operating current   20 A (60 A)
    Single-phase three-wire system   120 A (60 A)

4. Watt hour meter
    Operating voltage   110 V
    Measurable current range   0–5 A
    Measurable voltage range   60–260 V
    Maximum generation power measurement ratio range
                                       0 W–500 W/4 mA–20 mA (Single-phase two-wire system 110 V)
    Maximum load power measurement ratio range
                                       0 W–500 W/4 mA–20 mA (Single-phase three-wire system 220 V)
5. The amount of sunlight measurement   Pyranometer (made by EPLAB)
6. Temperature measurement   T-type Thermocouple
7. DC voltage measurement   FLUKE

8. DC current measurement   Shunts

9. AC voltage measurement   FLUKE

10. Frequency measurement   FLUKE

1.3 PV module structure and out looking evaluation

The PV system was installed on the third floor of the Construction Bureau of Penghu County Government in June 1999. The total area of the solar array is 23.32 square meter. The system can be grid-connected or off-grid connected, which offers 1.5 kilowatt AC (alternating current) electric power during day time. DC combiner box is installed at the array tripod corner. AC power panel, inverter, monitoring system, transformer, and watt hour meter, is installed on the first floor wall of the Civil Engineering Department. The system's parts were maintained/replaced in December 2007 to resume power output. Table1.3.1 lists Penghu system's specifications.

Manufacturer	Kyocera, Japan
Model	G421-3W
Date of manufacturing	1998.10
Pmax (W)	135 W
Voc	24.9 V
Isc	7.48 A
Vmp	19.5 V
Imp	6.92 A
Maximum system voltage	450 V

Table1.3.1 Penghu system's specifications

Figure 1.3.1 Overall view of the Penghu PV system

Figure 1.3.2 Module specifications of the Penghu PV system

Figure 1.3.3 Monitor display of the Penghu PV system

The Penghu PV system operated for 17 years under harsh environment. The aluminum frame had serious potential corrosion phenomena. When the system's parts were maintained/replaced in December 2007 to resume power output, plastic spacers were placed between aluminum frame and stainless screw to avoid potential corrosion. Figure1.3.4 shows that the mentioned action did not really solve the potential corrosion problem. It is suspected that the sea wind and rain with salt accumulated in the aluminum frame and screw. The accumulated salt became conductive and generate potential corrosion between the aluminum frame and screw.
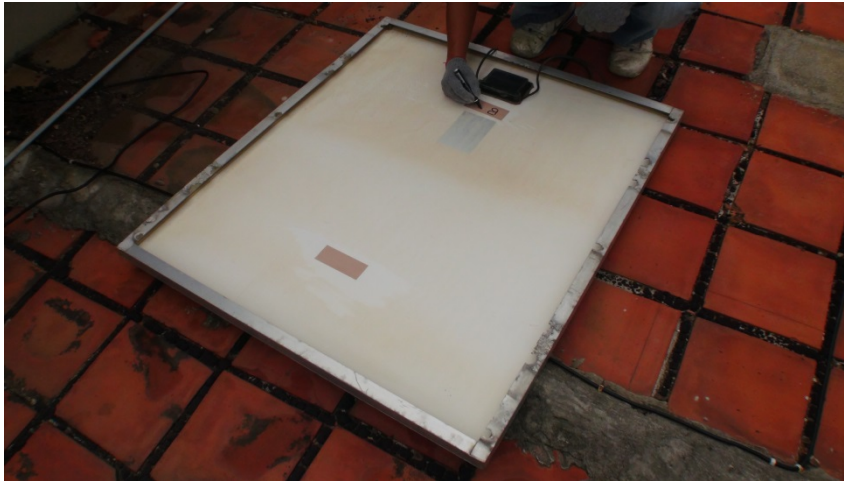
Figure 1.3.4 Aluminum frame with potential corrosion phenomena of the Penghu PV system

1.3.1 Module appearance structure inspection

First, inspection of the appearance of the modules structure was conducted. The inspection methods follow 10.1 Visual inspection of EC61215ed.2. The procedures are described in section 1.3.2.

1.3.2 Visual inspection

1.3.2.1 Purpose

To detect any visual defects in the module

1.3.2.2 Procedure

Carefully inspect each module under an illumination of not less than 1000 lux for the following conditions:

– Cracked, bent, misaligned or torn external surfaces;

– Broken cells;

– Cracked cells;

– Faulty interconnections or joints;

– Cells touching one another or the frame;

– Failure of adhesive bonds;

– Bubbles or delamination forming a continuous path between a cell and the edge of the module;

– Tacky surfaces of plastic materials;

– Faulty terminations, exposed live electrical parts;

– Any other conditions which may affect performance.

Make note of and/or photograph the nature and position of any cracks, bubbles or delaminations, etc, which may worsen and adversely affect the module performance in subsequent tests.

1.3.2.3 Requirements

Visual conditions other than the major visual defects listed in 1.3.2.4 are acceptable for the purposes of type approval.

1.3.2.4 Major visual defects

For the purposes of design qualification and type approval, the following are considered to be major visual defects:

a) Broken, cracked, or torn external surfaces, including superstrates, substrates, frames and junction boxes;

b) Bent or misaligned external surfaces, including superstrates, substrates, frames and junction boxes to the extent that the installation and/or operation of the module would be impaired;

c) A crack in a cell the propagation of which could remove more than 10% of that cell's area from the electrical circuit of the module;

d) Bubbles or delaminations forming a continuous path between any part of the electrical circuit and the edge of the module;

e) Loss of mechanical integrity, to the extent that the installation and/or operation of the module would be impaired.

1.3.2.5 Visual inspection results

Figure 1.3.2.5.1 Module number and relative position in the PV system

Module	Backsheet	Glass	EVA	Series cell	Junction box	Aluminum

No.	appearance	surface	encapsulation	connection	and Diode	frame appearance
A2	A* (very good)	Smooth surface Very good	Good connection without yellowing	Good connection	Diode burned out	C*
A3	4 corners defect (good)	Smooth surface Very good	Good connection without yellowing	Good connection	good	C*
A4	Upper corner defect (good)	Smooth surface Very good	Good connection without yellowing	Good connection	good	C*
A5	A* (very good)	Smooth surface Very good	Good connection without yellowing	Good connection	Diode burned out	C*
A6	Upper corner defect (good)	Smooth surface Very good	Good connection without yellowing	Good connection	good	C*
A7	B*	Smooth surface Very good	Good connection without yellowing	Good connection	good	C*
A8	B*	Smooth surface Very good	Good connection without yellowing	Good connection	Diode burned out	C*
A9	B*	Smooth surface Very good	Good connection without yellowing	Good connection	Diode burned out	C*
A10	B*	Smooth surface Very good	Good connection without yellowing	Good connection	good	C*

B1	Upper corner defect (serious)	Smooth surface Very good	Good connection without yellowing	Good connection	Diode burned out	C*
B2	B*	Smooth surface Very good	Good connection without yellowing	Good connection	good	C*
B3	B*	Smooth surface Very good	Good connection without yellowing	Good connection	Diode burned out	C*
B4	B*	Smooth surface Very good	Good connection without yellowing	Good connection	Diode burned out	C*
B5	B*	Smooth surface Very good	Good connection without yellowing	Good connection	Diode burned out	C*
B6	Aluminum foil oxidation (good)	Smooth surface Very good	Good connection without yellowing	Good connection	Diode burned out	C*
B7	A* (very good)	Smooth surface Very good	Good connection without yellowing	Good connection	Diode burned out	C*
B8	B*	Smooth surface Very good	Good connection without yellowing	Good connection	Diode burned out	C*
B9	Upper corner defect (serious)	Smooth surface Very good	Good connection without yellowing	Good connection	good	C*
B10	4 corners defect	Smooth surface	Good connection	Good connection	good	C*

	(good)	Very good	without yellowing			
B11	Upper corner defect (good)	Smooth surface Very good	Good connection without yellowing	Good connection	Diode burned out	C*

Table 1.3.2.5.1 Module visual inspection results

A*: welding repair between wider ribbon and long strip EVA & backsheet was used to strengthen the insulation of the module

B*: no situation need to be addressed

C*: pre-drilled holes for screw lock had serious potential corrosion

1.4 PV module performance and reliability evaluation

To study the long-term reliability of the PV system, which was located in the harsh coastal environment, 20 modules, operated in the Penghu area, were torn down and moved to Hsinchu laboratory for tests for maximum power, insulation, wet leakage current test, electroluminescence, thermal image temperature, etc.

1.4.1 Maximum power measurement of aging PV modules

The main purpose for maximum power measurement of aging the PV modules was to study the power decay after 17 years of operation in the harsh environment. Because the rated power is 135 W, if a given module can provide no less than 80% of the rated power, test was considered passed. Only 6 of 20 modules passed. The pass rate was 30%. The details are described below;

(Please see figure 1.3.2.5.1 which shows the module's number and related position in the aging PV system)

➢ 6 modules (A3, A4, A6, A9, B9, B10) passed and met the 80% requirement after 20 years of operation specifications.

➢ Module A7 reached close to 80% of rated power.

➢ 7 modules (A2, A5, A10, B1, B6, B7, B8) reached 50% of rated power.

➢ B11 reached 40% of rated power. Two series solar cells were not connected or had poor connection. Series solar cells may have worse defects.

➤ Power for modules A8, B2, B3, B4 could not be measured at all. The possible reasons were junction box that was disconnected or soldering failed in between wider ribbons.

Module No.	Pmax (W)	Umpp (V)	Impp (A)	Uoc (V)	Isc (A)	FF (%)	Rs	Rsh
A2	65.51	10.74	6.10	18.38	6.94	51.40	4.36	68.86
A3	107.91	18.33	5.89	24.73	6.92	63.01	0.63	58.57
A4	117.76	18.57	6.34	25.22	6.92	67.48	0.68	132.49
A5	63.19	11.33	5.58	16.33	6.93	55.84	1.21	11.24
A6	114.44	18.00	6.36	24.81	6.98	66.10	0.71	79.87
A7	103.62	17.19	6.03	24.73	6.92	60.54	0.86	139.80
A8	0.00	0.00	0.00	0.00	0.00	0.00	0.00	0.00
A9	118.17	18.50	6.39	24.83	6.87	69.26	0.75	120.69
A10	67.86	10.95	6.20	24.86	6.87	39.76	12.18	98.55
B1	62.43	10.80	5.78	23.29	6.81	39.37	10.74	34.23
B2	0.00	0.00	0.00	0.00	0.00	0.00	0.00	0.00
B3	3.62	2.08	1.74	16.37	0.88	25.04	76.75	4.85
B4	0.00	0.00	0.00	7.13	0.00	0.00	56583	0.00
B5	17.60	3.63	4.85	14.42	6.84	17.83	24.49	1.17
B6	63.97	10.52	6.08	22.56	6.83	41.49	10.01	78.52
B7	65.49	10.61	6.17	16.96	6.80	56.76	2.58	88.78
B8	67.49	10.87	6.21	23.85	6.88	41.11	11.27	90.61
B9	111.12	17.81	6.24	25.09	7.05	62.82	0.97	34.78
B10	118.10	18.83	6.27	24.81	6.88	69.23	0.61	139.52
B11	55.92	9.41	5.95	24.78	6.84	32.97	13.03	30.42

Table 1.4.1.1 maximum power measurement of Penghu PV modules

1.4.2 Insulation test and wet leakage current test of aging PV modules

After the insulation test and wet leakage current test of aging PV modules, it was found that only two modules did not pass the test. Module A7 had poor silicon glue in

the junction box. The junction, therefore, was leaking. The root cause for module A10 was delamination or formation of conducting path between solar cell and glass.

Module No.	Specification (MΩ·m²)	Insulation test (MΩ·m²)	Wet leakage current test (MΩ·m²)	Status
A2	43	603	295	pass
A3	43	837	268	pass
A4	43	718	352	pass
A5	43	802	275	pass
A6	43	371	100	pass
A7	43	1321	15	disqualify
A8	43	856	183	pass
A9	43	2558	290	pass
A10	43	6	X	disqualify
B1	43	537	312	pass
B2	43	1025	337	pass
B3	43	856	453	pass
B4	43	680	359	pass
B5	43	609	313	pass
B6	43	605	314	pass
B7	43	861	343	pass
B8	43	636	295	pass

B9	43	569	323	pass
B10	43	515	296	pass
B11	43	616	272	pass

Table 1.4.2.1 Insulation test and wet leakage current test of Penghu PV modules

1.4.3 Spectral characteristics detection of the Penghu PV module

Backsheet's reflectivity measurement
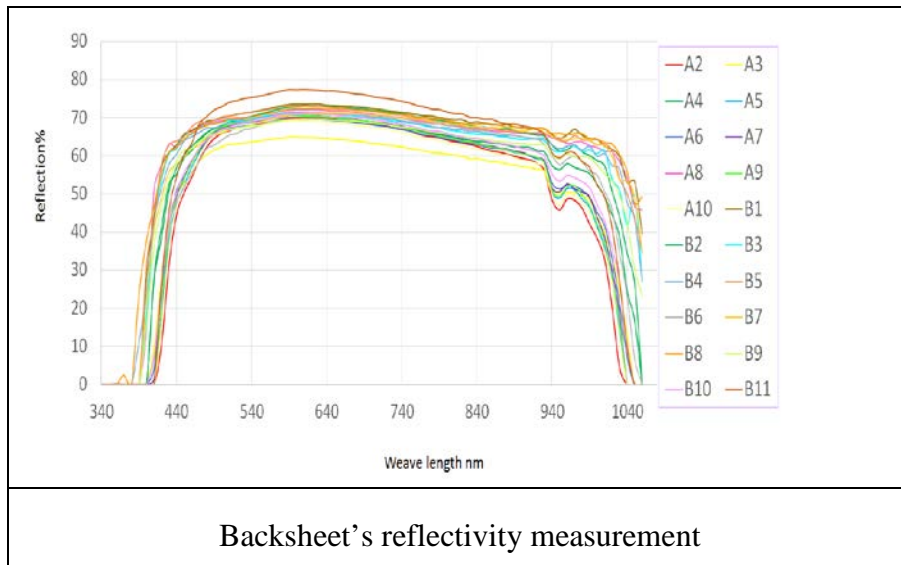
Figure 1.4.3.1 The Spectral characteristics detection of Penghu PV module

The main purpose for the spectral characteristics detection of the aging PV module was to know the aging status of the backsheet. Backsheet exposure in the sun and long term thermal cycle resulted in yellowing and aging phenomena after 17 years in operation. The aging modules still had around 65–75% reflectivity. Yellowing was not serious. It is mean that the quality of the backsheet materials is good.

1.4.4 Electroluminescence detection of the Penghu PV module

3.5 A and 7.5 A current were used for EL (Electroluminescence) detection of the aging modules. EL picture was clear for 7.5 A current. Some modules showed no EL detection picture because the electric current was not turned on. Although ome solar cell showed darker EL picture in all modules, the power was still 107.91 W. The detailed description of the EL detection results are below:

➢ Modules A7 and A9 had broken solar cells inside.

➢ Module A2: one of two Busbar had better conductivity, resulting in brighter EL picture (whiter in the picture).

➢ Module A3: some solar cell had poor power, resulting in darker EL picture (blacker in the picture).

A4	
3.5A	7.5A

A6	
3.5A	7.5A

A7	
3.5A	7.5A
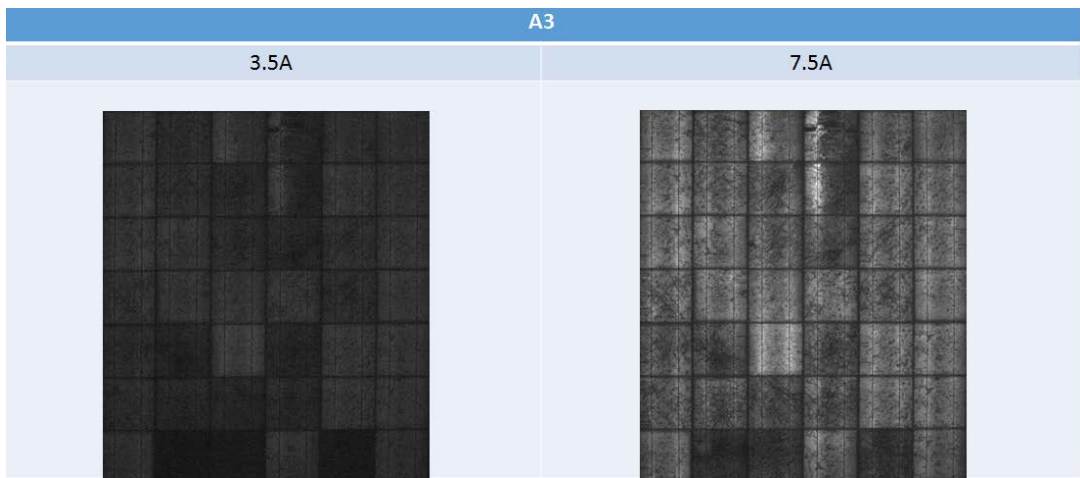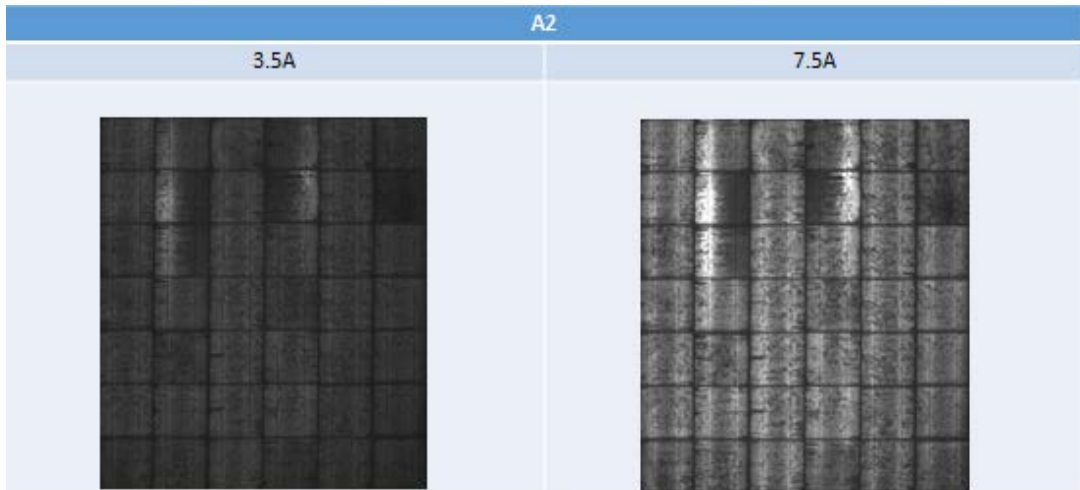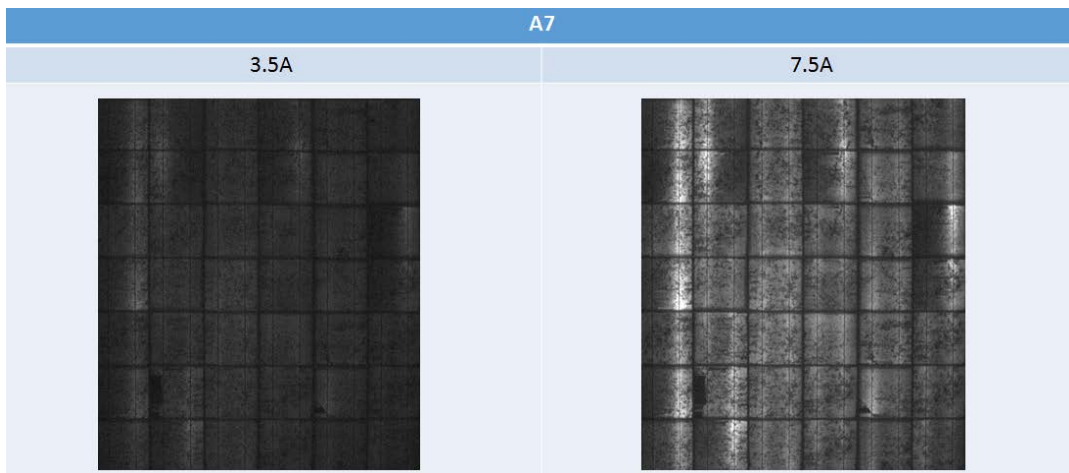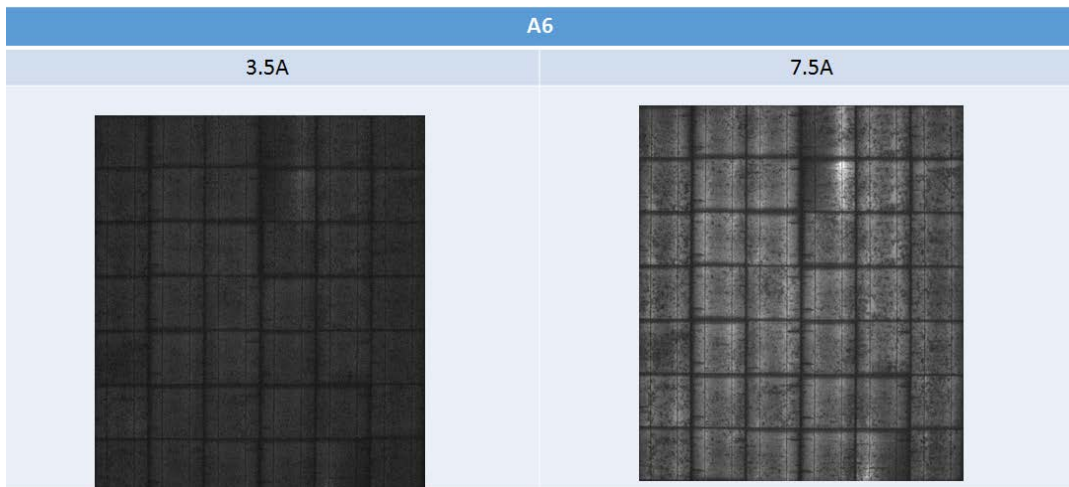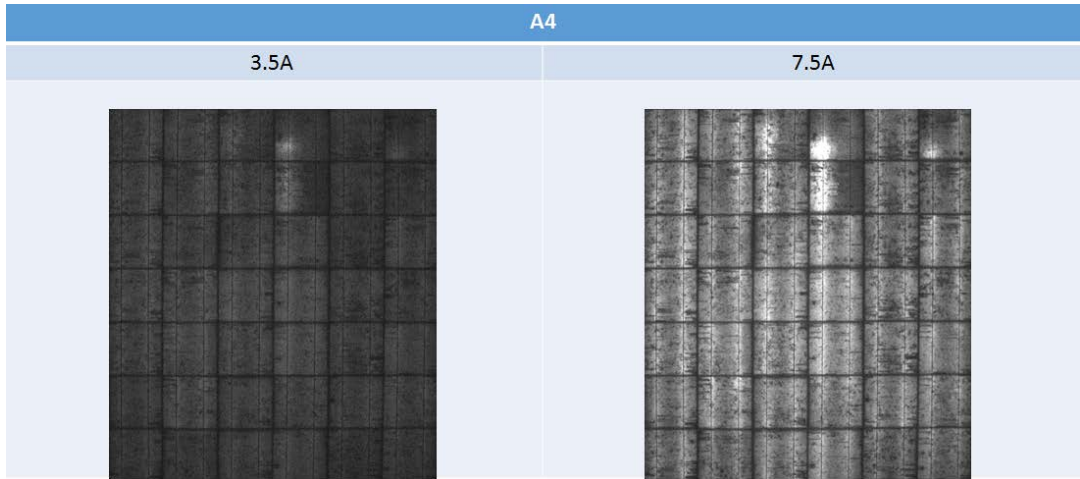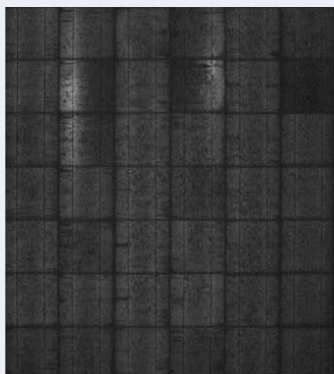
A9	
3.5A	7.5A
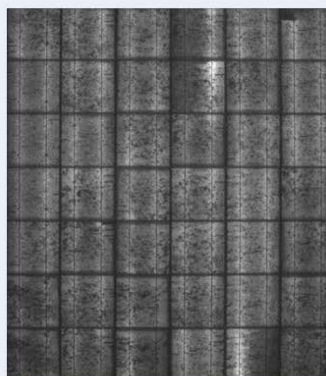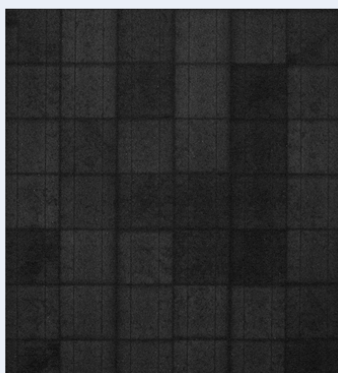
B1	
3.5A	7.5A
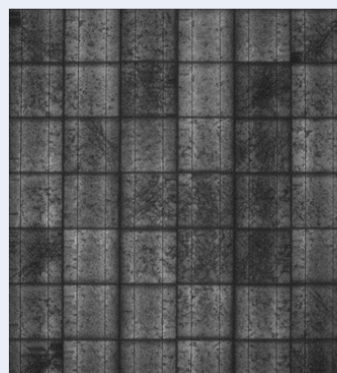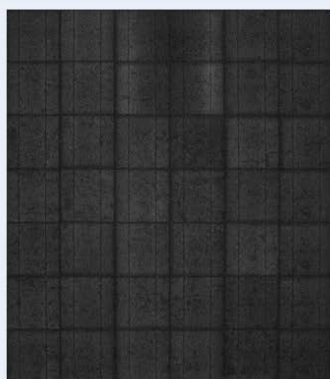
B6	
3.5A	7.5A
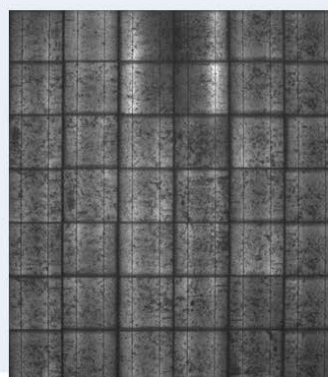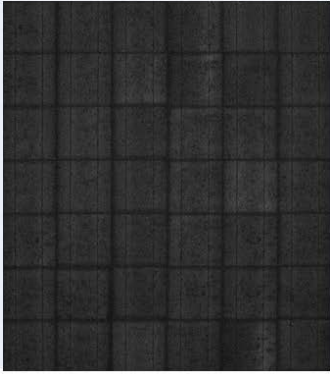
B8	
3.5A	7.5A
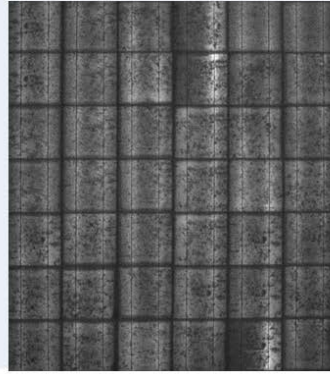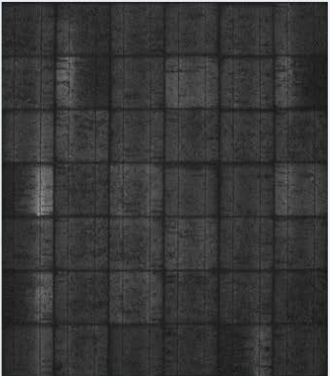
B9	
3.5A	7.5A
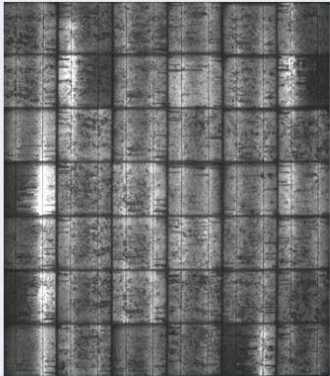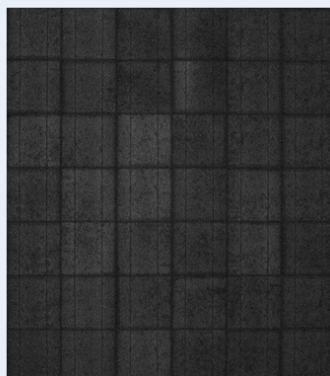
B10	
3.5A	7.5A
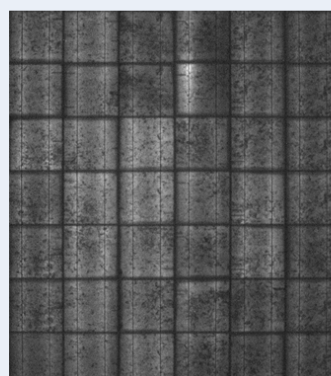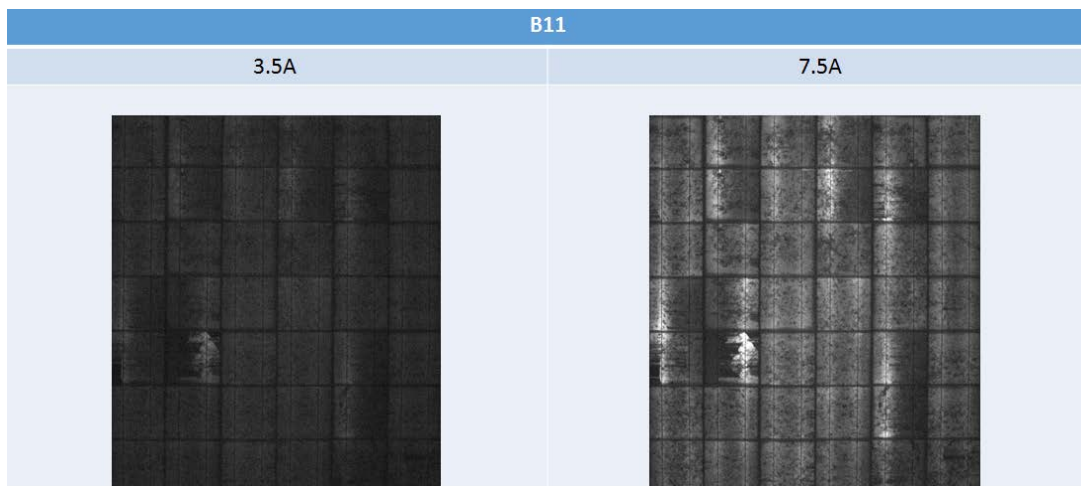
Figure 1.4.4.1 EL results of the Penghu PV modules

模組編號	A2	A3	A4	A6	A7	A9	B1	B6	B8	B9	B10	B11
3.5A	26.51	25.49	26.54	25.87	26.31	26.62	26.06	27.81	25.55	26.61	26.13	26.25
7.5A	30.55	28.95	30.05	29.07	30.22	29.18	29.01	31.34	28.68	30.04	28.84	29.62
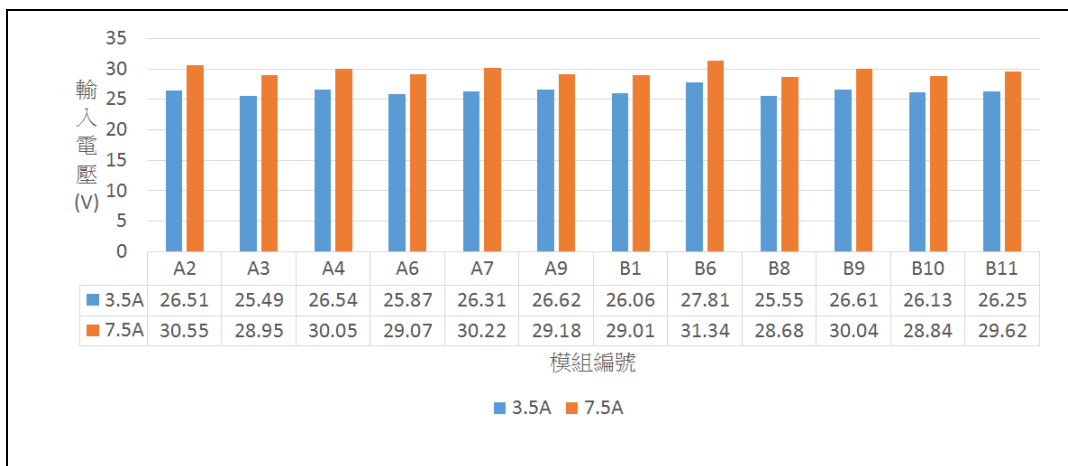
Figure 1.4.4.2 EL results of the Penghu PV modules-electric voltage relationship

Whenever EL used the same current to turn on the electric path, higher voltage means poorer module condition. Module B6 was typical of a module in poorer condition.

1.4.5 Infrared thermal image of the Penghu PV module

The main purpose for the infrared thermal image of the aging PV module is to find the hot spot of modules. The test results show that the highest temperature is 33.5°C. Because the frame is too close to solar cell, residual rain and dust may cause shedding and form the hot spot phenomena. Module A9 showed the highest temperature, 33.5°C, the root cause of this phenomenon is because the solar cell broke after comparison with EL results.
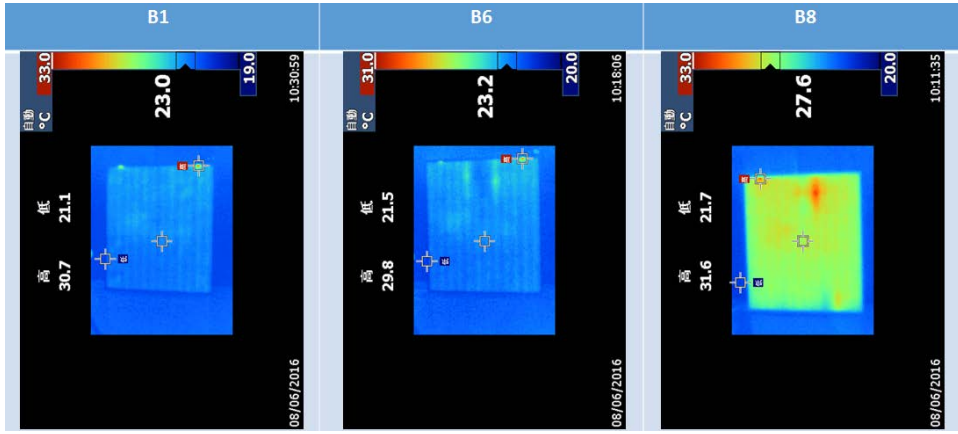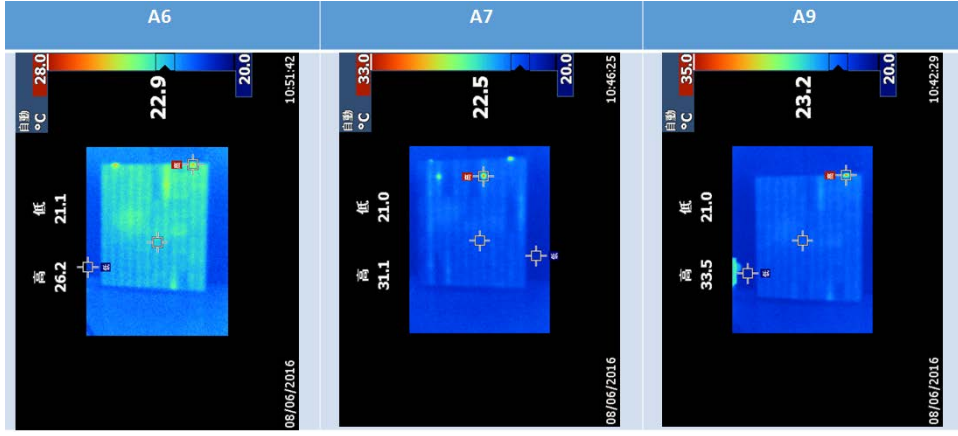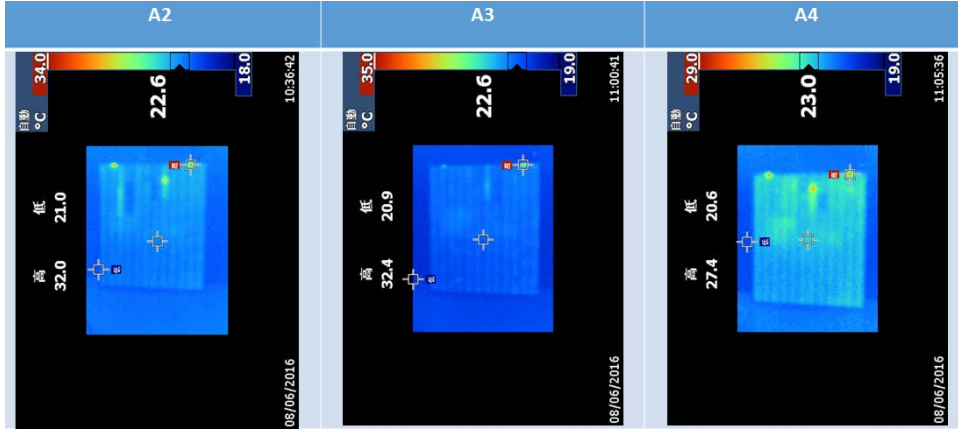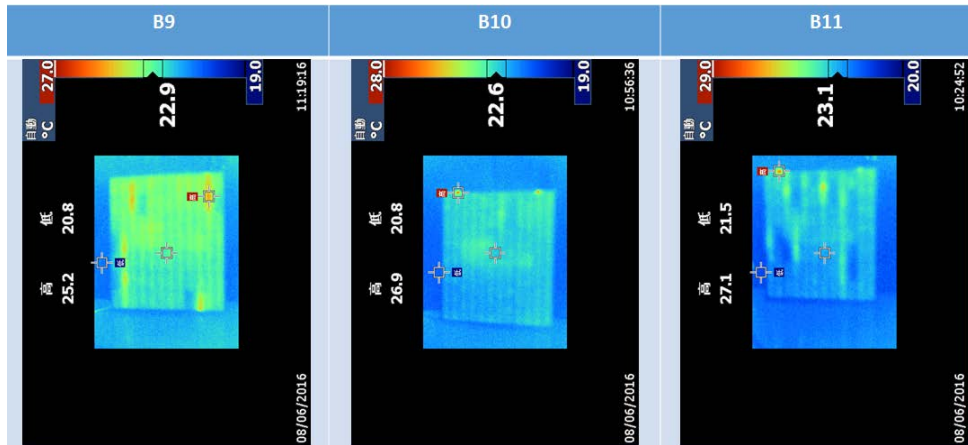
Figure 1.4.5.1 The Infrared thermal image of Penghu PV module

模組編號	A2	A3	A4	A6	A7	A9	B1	B6	B8	B9	B10	B11
最高溫	32	32.4	27.4	26.2	31.1	33.5	30.7	29.8	31.6	25.2	26.2	27.1
最低溫	21	20.9	20.6	21.1	21	21	21.1	21.5	21.7	20.8	20.8	21.5
平均溫度	26.5	26.65	24	23.65	26.05	27.25	25.9	25.65	26.65	23	23.5	24.3
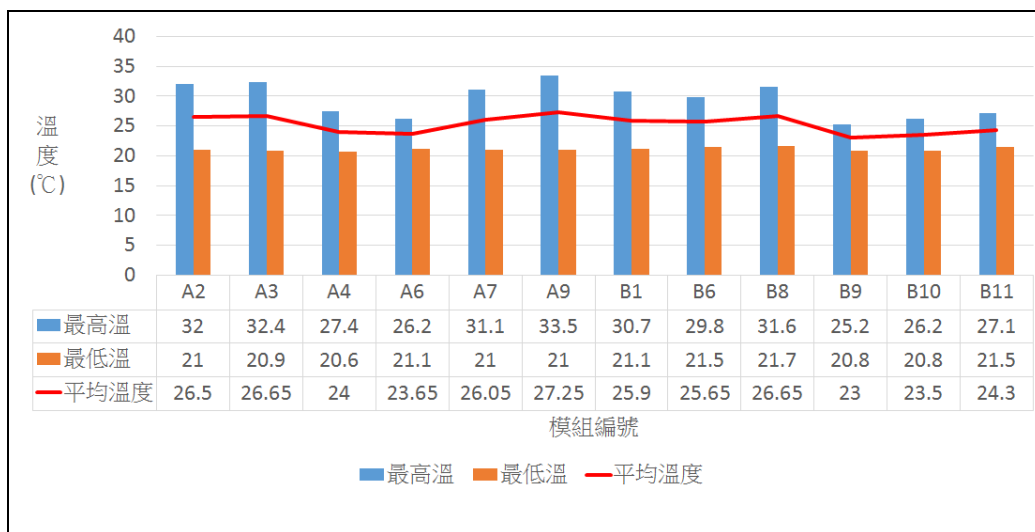
Figure 1.4.5.2 Infrared thermal image of Penghu PV module-temperature relationship

　　：highest temperature

　　：lowest temperature

　　：average temperature

1.5 Failure mode analysis of the aging PV module

1.5.1 Potential corrosion of the aging aluminum frame

1.5.1.1 Status description

Potential corrosion was found at the lock screw position of the aging Penghu PV system. The pre-drilled holes for lock screws all collapsed. It was a problem for all 20 modules in the aging PV system.

1.5.1.2 Root cause analysis

The typical process sequence of the aluminum frame was first to do the anodic treatment and then pre-drilled holes for lock screws. The holes, therefore, did not have anodic treatment. Stainless screws were used to lock modules in the aluminum frame. Although plastic spacers were used between aluminum frame and screw, the insulation performance is not good. The potential difference between the aluminum frame and the screw results in potential corrosion. It is possible that the salt in the air accumulates in the pre-drilled holes. The accumulated salt becomes conductive resulting in potential corrosion.

1.5.1.3 Potential strategy for improvement

For the new aluminum frame, pre-drilled holes were processed before going through anodic treatment. In other words, all pre-drilled holes had anodic treatment.

Figure 1.5.1.3.1 pre-drilled holes of aluminum frame

Left: potential corrosion found at the pre-drilled holes of the aluminum frame.

Right: all pre-drilled holes with anodic treatment for the new aluminum frame.

1.5.2 Diode inside junction box burned out

1.5.2.1 Status description

Twelve of 20 diodes inside junction boxes burned out.

1.5.2.2 Root cause analysis

The solar cell inside each module should be connected by a thin ribbon. Wider ribbons were used to connect series solar cells and junction, which was located at the back of each module. The poor connection between wider ribbons resulted in high resistance and burned out the diode.

1.5.2.3 Strategy for diode burn out improvement

It is a necessary connection between wider ribbons due to the connection structure of the aging module. Tin/lead wire was used to reinforce the strength of the ribbon connection. Expansion caused by heat and contraction caused by cold is the root cause of the poor connection between wider ribbon. The chosen diode should pass the bypass diode thermal test of IEC61215ed.2.

Figure 1.5.2.3.1 Junction box inside parts/structure

Left: diode burn out; center: normal diode of aging module; right: replaced new junction box

1.5.3 Wider ribbon of aging PV system shedding results in power loss of the

system

1.5.3.1 Status description

Figure 1.5.3.3.1 shows the connection position between wider ribbons. The shedding or poor connection between wider ribbons resulted in no power output or loss of one or two series solar cell power, respectively. Thirteen of 20 aging modules were damaged.
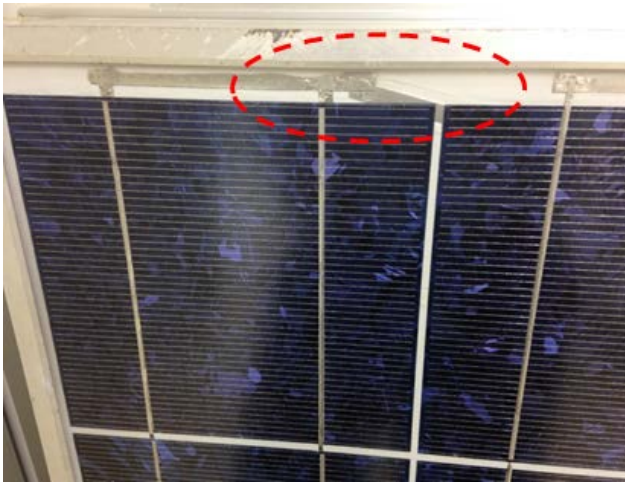
Figure 1.5.3.1.1 Shedding position of wider ribbons

1.5.3.2 The root cause of power loss

It is suspected that wider ribbons were connected through simple hot melt process. Since the connection point lacked tin/lead, the connection was not melt into one. Shedding will happen whenever EVA and backsheet encounter expansion caused by heat and contraction caused by cold

1.5.3.3 Strategy for wider ribbon shedding improvement

Tin/lead wire should be used to reinforce the strength of ribbon connection. The reinforced connection point therefore can stand expansion caused by heat and contraction caused by cold cycles.

2 The Interface failure modes among PV module materials

2.1 Exanimating the interface of PV module

2.1.1 Solder for ribbon Analysis

Currently, the solder used for welding the ribbon in PV system are diverse. The main components of solder were tin and lead with small amounts of other components, such as silver, bismuth, and indium. The lowest melting point of commercial solder, 183°C, is composed of Sn63/Pb36/Ag2. There is no pasty state between liquid (melting temperature) and solid (freezing temperature). The solder is called eutectic alloy, because the alloy forms a homogeneous solid mix (with tin and lead). The Tensile strength of eutectic Sn63/Pb37 alloy ("63/37" in the following) at welding point is 7250 PSI at room temperature. The shear strength of alloy has more effect on the properties of the solder joint. Antimony is typically added to tin–lead solder to replace the more expensive tin, to reduce the cost of soldering and to augment the mechanical and ductility properties of the solder joint. The ductility and elastic modulus of 63/37 is better than that of Sn/Pb composition, high melting point alloy. The thermal and electric conductivity of alloy is poorer than that of pure tin. The mentioned conductivity slightly decreases by adding lead. In general, the mechanical properties of 63/37 were better than that of other Sn/Pb alloy. Increasing tin enhances the mechanical properties of a given alloy. Sn60/Pb40 is other composition, which has property close to eutectic alloy, and is widely used in the electronic industry due to the high cost of tin. The solder ability and joint strength of both eutectic alloys are similar to each other. Decreasing tin by 3%, hopefully, will reduce cost.

The PV system has been in operation for more than 17 years at Penghu Island's harsh hot and humid environment. After dismantling the PV module, the EVA showed no corrosive phenomenon. It indicates that the quality of both EVA and backsheet are good. In other words, no cracking acetic acid or small molecular was found. For the backsheet, low humidity penetration of backsheet evaded corrosion. The requirements of the ribbon properties will be analyzed and discussed in the following sections.

2.1.1.1 Ribbon resistance measurement

The resistance is measured by 4-point probe following CNS5745 measurement method. The results are shown in Figure 2.1.1.1. As mentioned previously, Kyocera modules are used in the PV system in Penghu Islands, which has been in operation for more than 16 years. A company mean that the ribbon is brand new without having been used. It is clear that the used ribbon has higher electrical resistance.
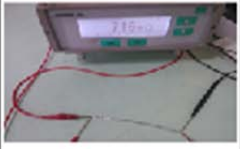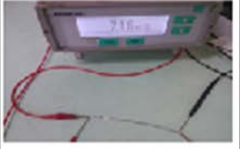
	Kyocera Module		A Company	
	Cell Ribbon(14cm)	Bus Ribbon(12cm)	Cell Ribbon(14cm)	Bus Ribbon(12cm)
Composition(%)	Sn 64.1% / Pb 35.9%	Sn 63.4% / Pb 36.6%	Sn 63.7% / Pb 36.3%	Sn 64.4% / Pb 35.6%
Resistance (mΩ)	7.16	1.79	5.88	0.87
Note				

Figure 2.1.1.1Comparision of used and brand new ribbon electric resistance

2.1.1.2 Ribbon dimension and coated metal thickness measurement

The measurement results of ribbon dimension and coated tin/lead alloy thickness on the surface of ribbon are listed in table 2.1.1.2. The tin/lead alloy coating on the surface of ribbon of Kyocera modules is thicker than that of current commercial/domestic brand A. The coating uniformity, which affects the stability and operability of welding, of the Kyocera module is good.

Item	Kyocera Module		Company A (main domestic brand)	
	Cell ribbon	Bus ribbon	Cell ribbon	Bus ribbon
Ribbon width (mm)	2.051	5.984	1.963	5.947
Ribbon thickness (mm)	N/A	0.386	0.247	0.439
A Side coating thickness (□m) (Tin & lead alloy)	36.3	37.5	20.6	21.0
	35.0	38.3	21.5	18.9
	28.5	33.1	21.9	20.7
Average	33.3	36.3	21.3	20.2
B Side Coating Thickness(□m) (Tin & lead alloy)	30.7	30.1	16.7	21.3
	36.8	26.6	18.1	19.7
	31.4	33.1	16.7	19.6

Average	32.9	23.6	17.2	20.2

Table 2.1.1.2 Measurement results of ribbon dimension and coated tin/lead alloy thickness

2.1.1.3 Element analysis of used ribbon in the Penghu PV system

Energy Dispersive Spectrometer (EDS) in scanning electron microscope (SEM) was used to analyze the elements of used ribbon in the Penghu PV system. After EDS analysis, the tin/lead ratio is about 66/34 and 68/32 for thinner ribbon (connecting solar cell) and wider ribbon (connecting series cell and junction box) respectively.

Spectrum processing : No peaks omitted Processing option : All elements analyzed (Normalised) Number of iterations = 2 Standard : Sn Sn 1-Jun-1999 12:00 AM Pb PbF2 1-Jun-1999 12:00 AM Elem... Weight% Atomic% Sn L 66.35 77.49 Pb M 33.65 22.51 Totals 100.00 Comment:	EDS for cell ribbon
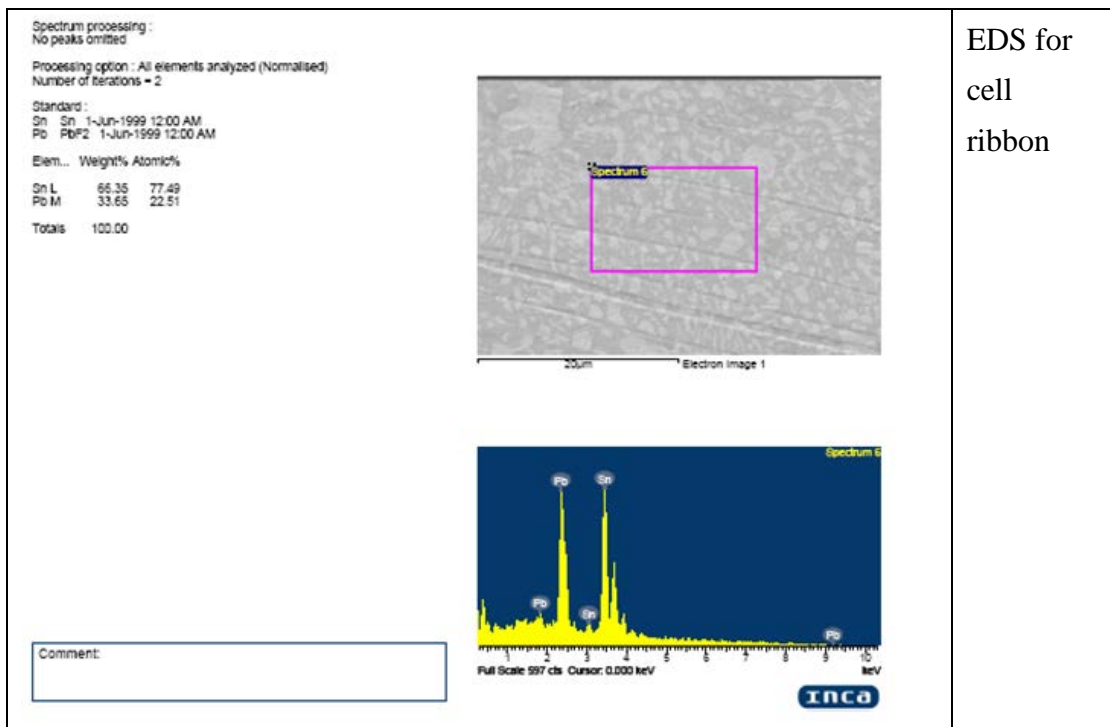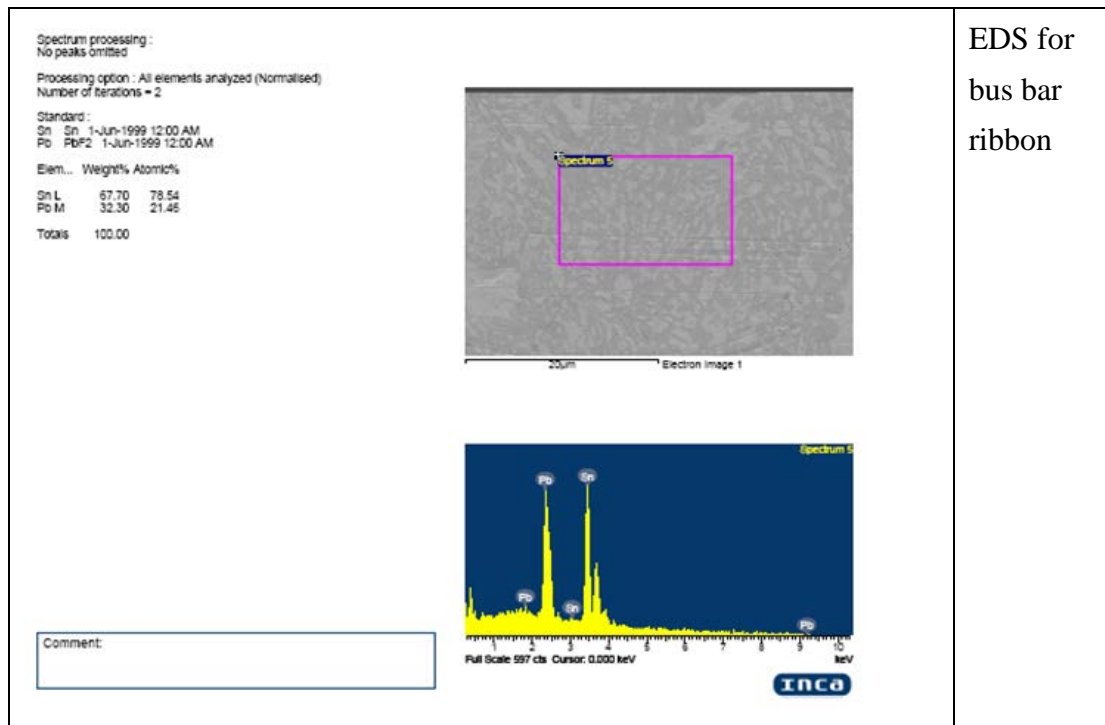
Figure 2.1.1.3 Element analysis of the used ribbon in the Penghu PV system

2.1.2 Silver and aluminum pastes used in the Penghu PV system analysis

Solar cells are 'tuned' to specific wavelengths, visible light, of light into electric power through photoelectric effect (production of electrons or other free carriers when light is shone onto a material). A semiconductor material/solar cell, typically, absorbs a photon and creates an exciton (an electron-hole) pair. To create an exciton, certain minimum energy is required. A photon having this energy will be absorbed, not any lower ones. The conductivity of silver and aluminum paste affect the conversion efficiency of a given solar cell because the light excited free electrons and holes are separated at the depletion region (built-in electric field) at P-N junction and then collected by electrode. Figure 2.1.2.1 shows that the finger in the front of solar cell do not see any "broken line" and corrosive phenomenon after operating for more than 17 years. The phenomenon is related to the quality of EVA materials. The EVA material is still transparent without yellowing (low acetate release/decompose).

Filler, typically white in color, is added into EVA for the application of solar cell back side encapsulation. Figure 2.1.2.2 shows leaf-shaped finger, which is especially designed. The figure is taken after removal of Backsheet and EVA. The fingers also do not see any "broken line" and corrosive phenomenon.

Figure 2.1.2.1 Finger in the front of module

Figure 2.1.2.2 Finger in the back of module

2.1.3 EVA analysis

EVA (Ethylene-vinyl acetate) not only enhances power generation efficiency, but also protects a given solar module, increasing the service cycle of a given solar module. EVA is a thermosetting plastic. EVA becomes transparent with good light penetration capability after curing. EVA, a key component of solar module, "glue" the

top and bottom glasses to form a protection structure for the module.

Light transmittance is a key index to judge whether EVA maintains high light transmission under corrosive environment and yellowing phenomena of a given EVA. Spectrophotometer (Hitachi U-4100 double monochromator UV-VIS-NIR) is used to measure the light transmittance of EVA samples. It is well reported that the decaying light transmittance of a given EVA present with serious yellowing. The failure mode results in decreasing power generation of a given module. Improving yellowing and electrical volume resistivity help enhance a given PV system's overall performance under corrosive environment.

Aging EVA (taken from the Penghu PV system) and brand new EVA are analyzed by FTIR (Fourier transform infrared spectroscopy) to know more about EVA failure mode. Figure 2.1.3.1-2.1.3.4 shows that both top and bottom encapsulation film are EVA after the library search of FTIR. The acetate's, 1735 cm^{-1} peak at FTIR, C=O bond strength clearly decreased for the aging film. It means that acetic acid decomposed and freed. Also, peak at 1716 cm^{-1}, which represent by-products such as aldehyde and ketone, is stronger than that of brand new EVA. It is clear evidence that the EVA inside aging module is cracking. FTIR effetely analyzed EVA's yellowing phenomenon, cracking acetic acid and formation of aldehyde and ketone by-products. New peak at 3400, 1645 and 1540cm^{-1} is found. After further analysis, OH bond for water, peak at 3400cm^{-1}, is found. Polyene bond, peak at 1645 and 1540 cm^{-1}, is also found. It can be concluded that aging EVA has more water content, yellowing, and acetic acid precipitation. All factors, such as module corrosion, increasing series resistance, acetic acid precipitation, and yellowing EVA, result in a reduction in the amount of incident light, and finally affect module service life and output power after operating for 17 years in Penghu Islands.
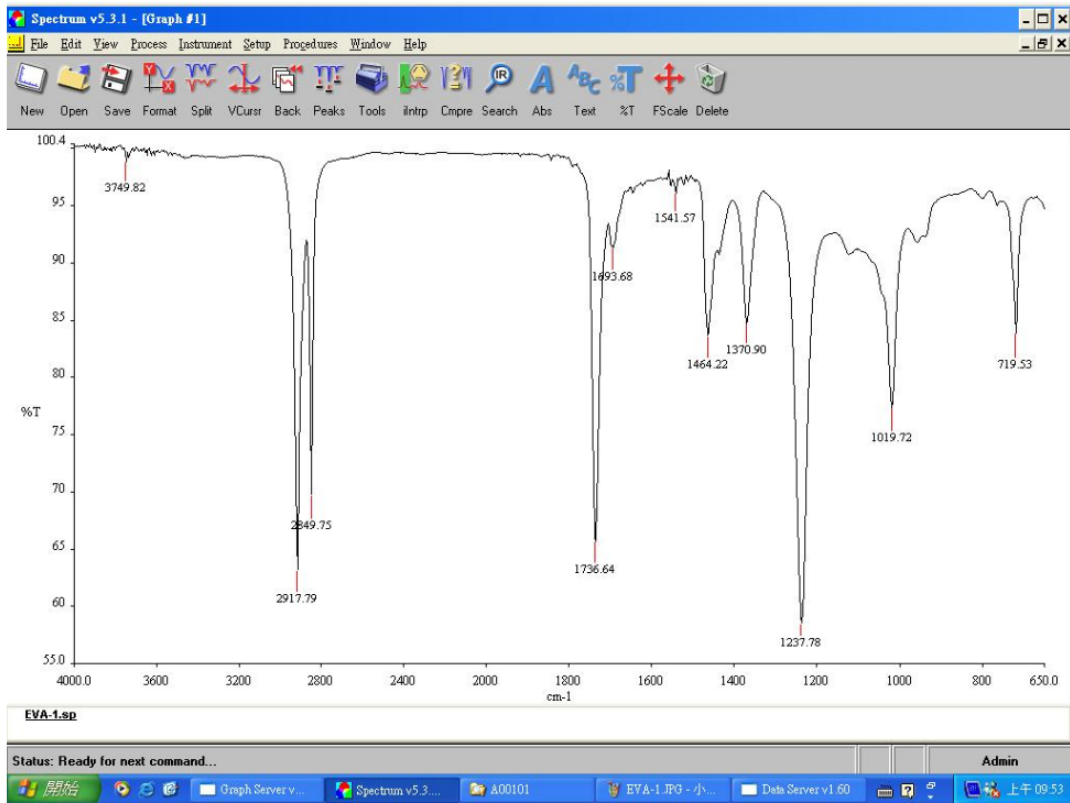
Figure 2.1.3.1 FTIR analysis of the top encapsulation film of the aging module
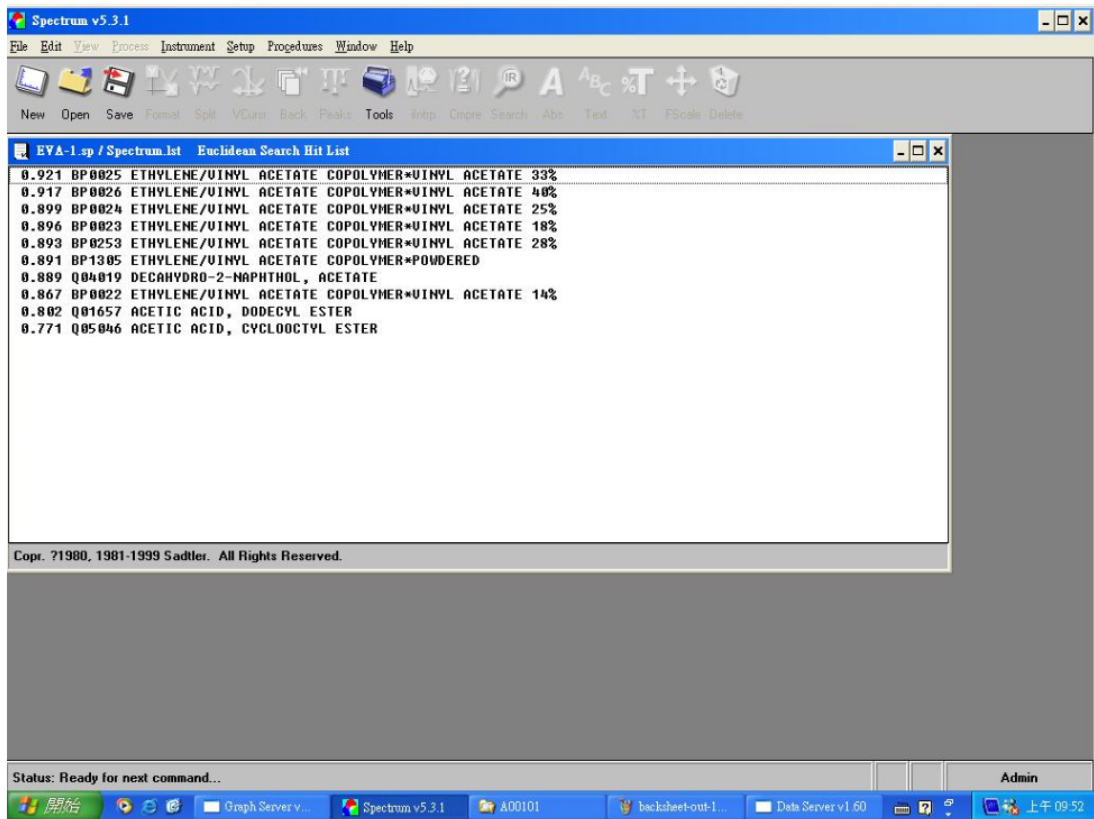
Figure 2.1.3.2 FTIR's library search analysis of the top encapsulation film of the aging module
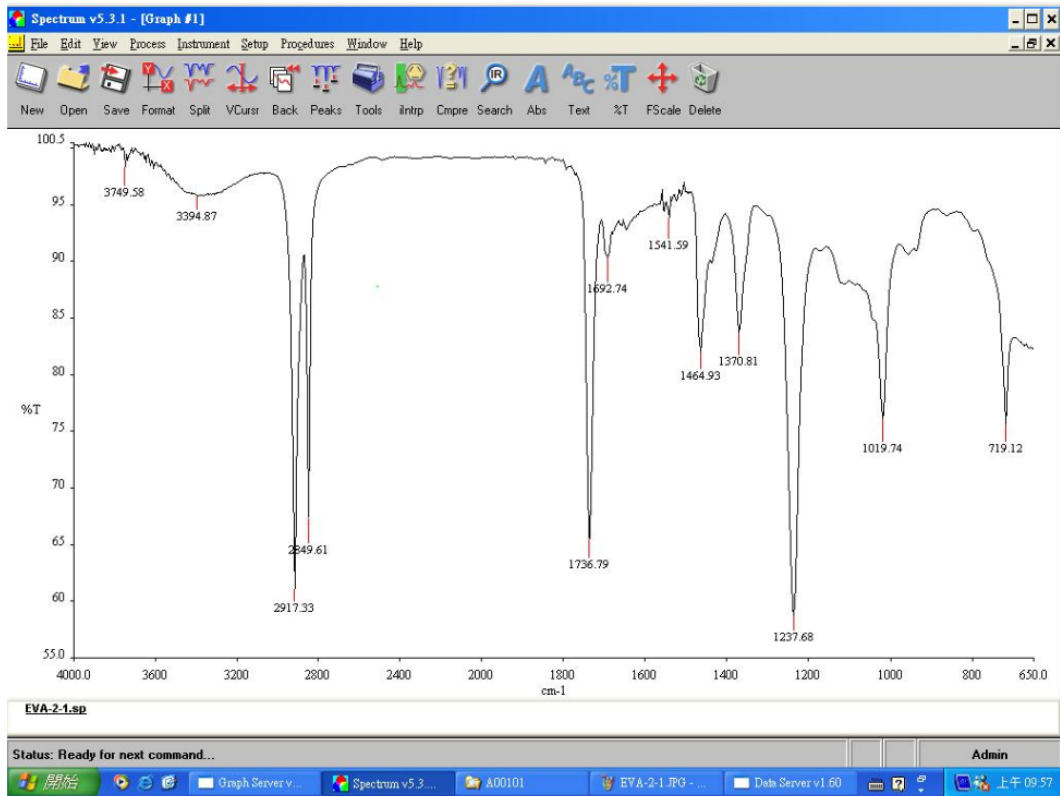
Figure 2.1.3.3 FTIR analysis of the bottom encapsulation film of the aging module
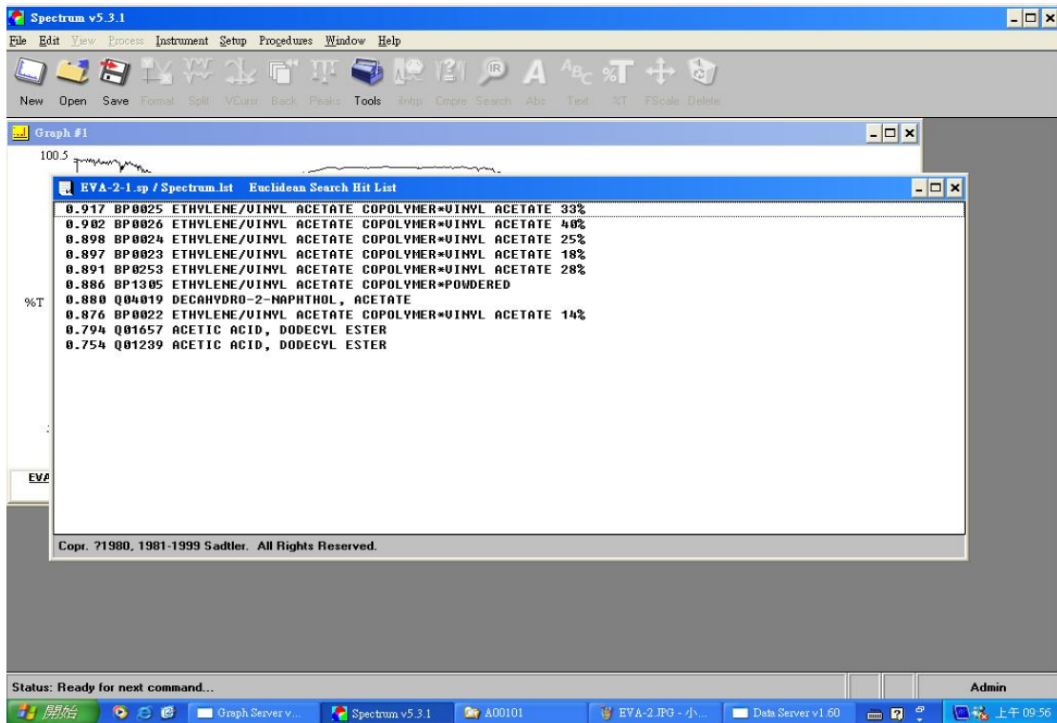
Figure 2.1.3.4 FTIR's Library search analysis of the bottom encapsulation film of the aging module
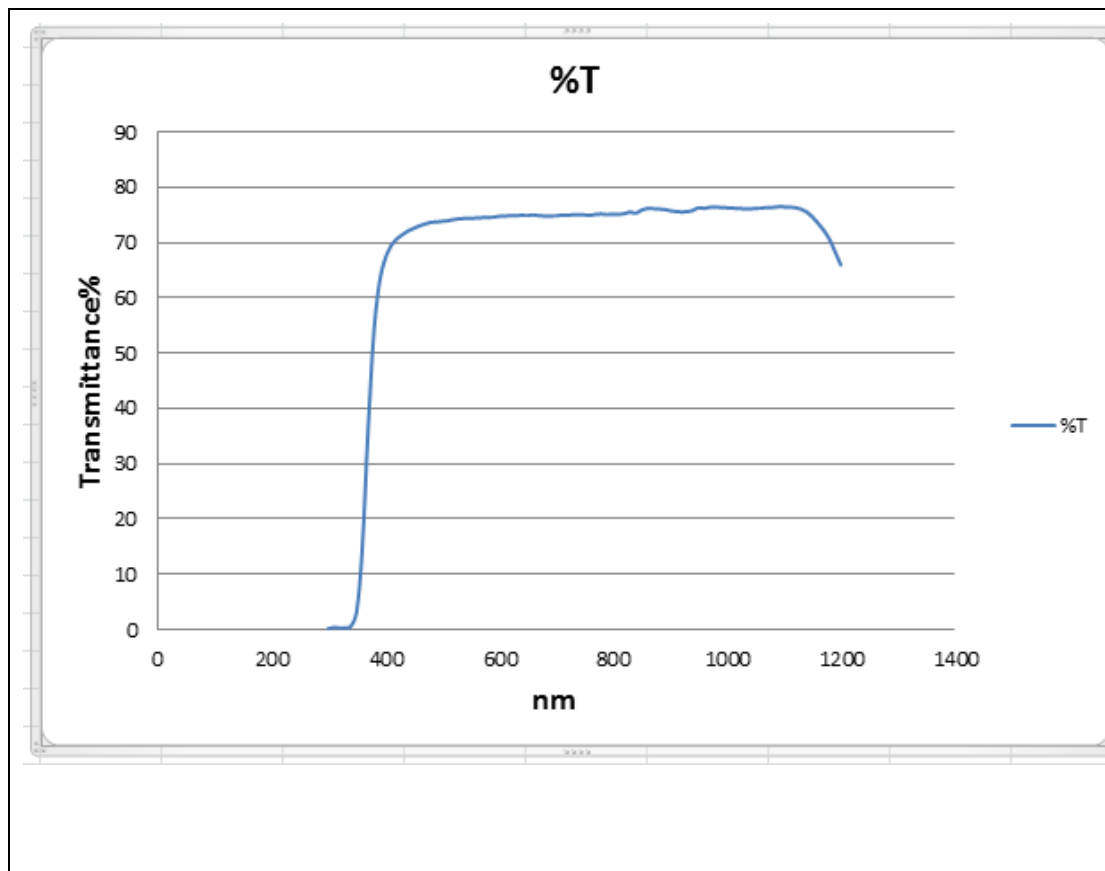
Figure 2.1.3.5 FTIR analysis-light transmittance of the top encapsulation film of the aging module

Figure 2.1.3.5 show that the light transmittance of the top EVA of the aging module is 75%. The value is far below the typical 88–90% for brand new EVA. The value indicates that the EVA in the aging module has aging phenomenon without yellowing. The bottom EVA of the aging module is still white. It means that the added filler, titanium dioxide, is still good after operating for 17 years in Penghu Islands.

2.1.4 Backsheet analysis

Backsheet's main function is to protect the back side of a given module. Backsheet blocks humidity, keeping the solar module from being attacked by weather. Also, the white color reflects light into cell to enhance the power output of the module. The typical structure of backsheet is Tedlar /PET / Tedlar. Tedlar ((Poly(Vinyl Fluoride, PVF)) is the commercial name of the DuPont product. DuPont invented the material in 1940. PVF offers excellent toughness and durability. PET (PolyEthylene

Terephthalate) has excellent hydrolysis resistance, insulation, reflectivity, UV

protection, and durability.
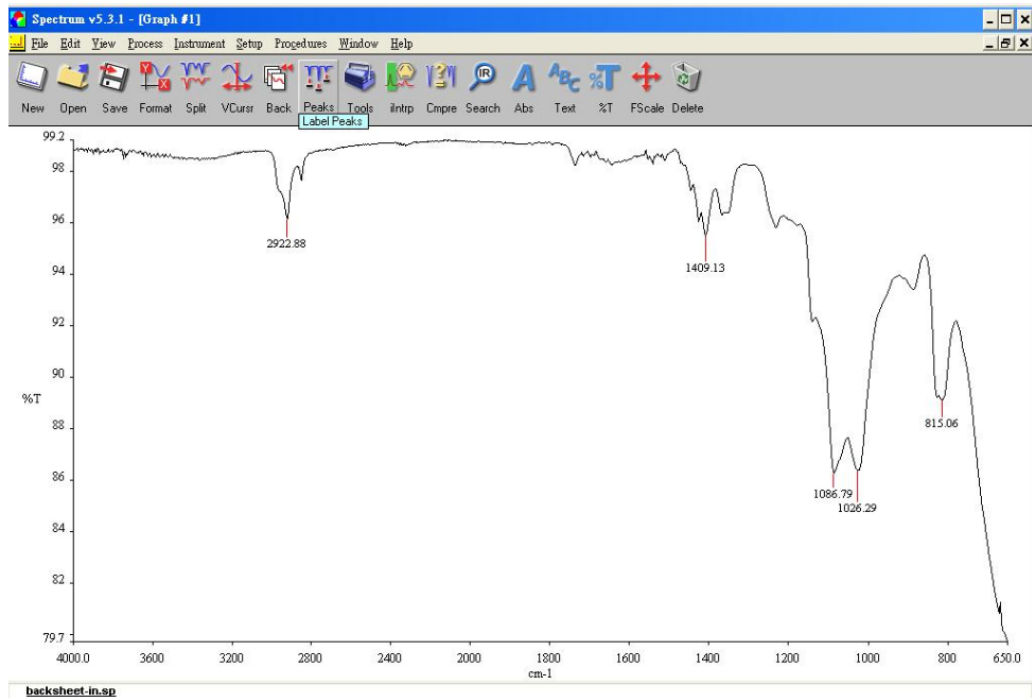
Figure 2.1.4.1 FTIR confirms that the inner layer of the aging backsheet is PVF film
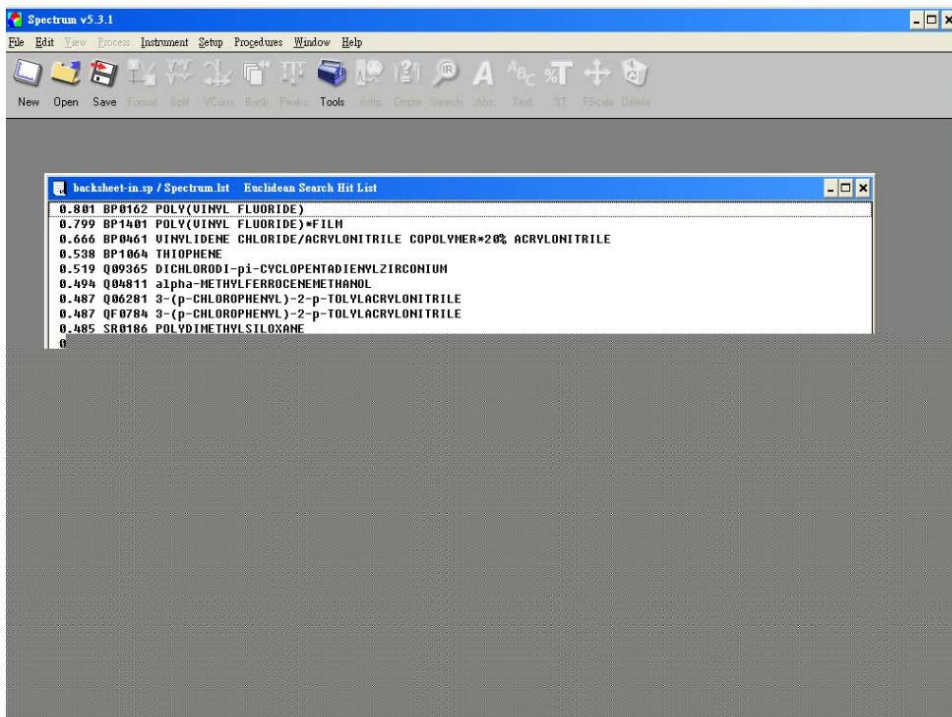
Figure 2.1.4.2 FTIR Library search shows that the inner layer of aging

Backsheet is PVF film
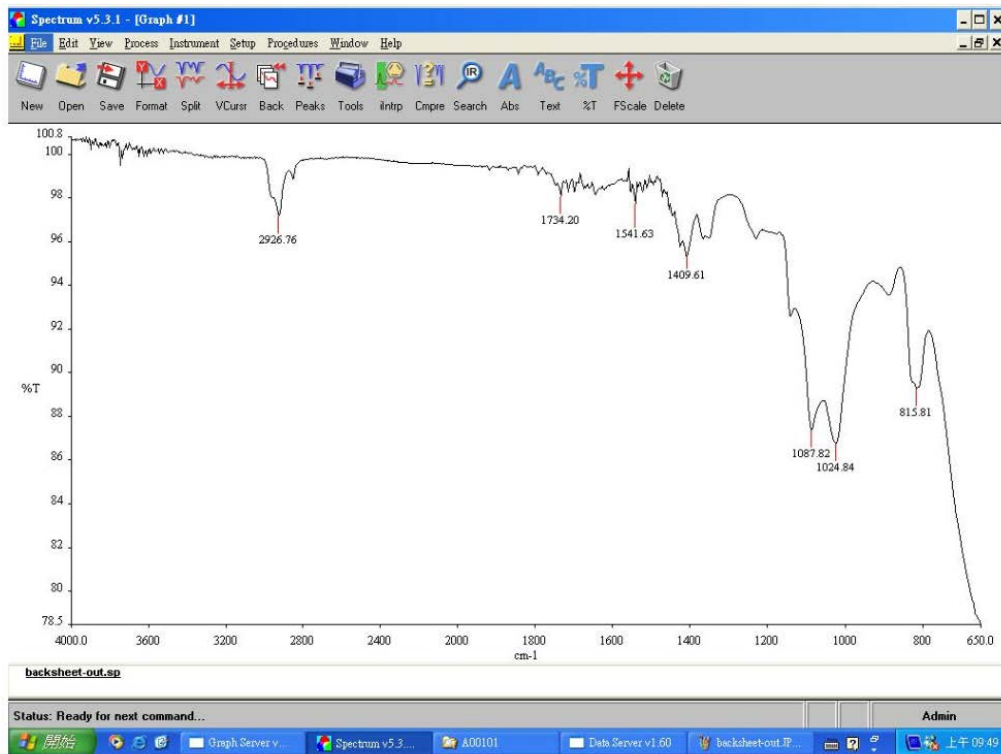
Figure 2.1.4.3 FTIR confirms that the outer layer of aging Backsheet is PVF film
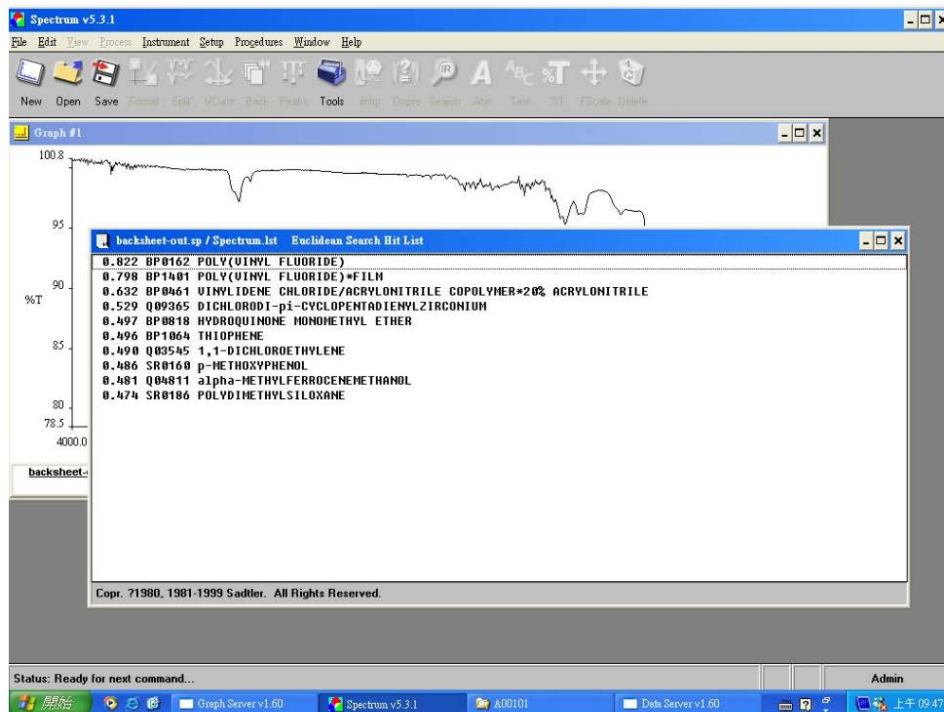
Figure 2.1.4.4 FTIR Library search shows that the outer layer of aging backsheet is PVF film

The aging backsheet (taken from Penghu's PV system) has a four-layer structure. After FTIR analysis, it is confirmed that PVF (Polyvinyl fluoride) film from DuPont was used. The structures from inner to outer layers are PVF (Polyvinyl fluoride)/PET/aluminum film/ PVF (Polyvinyl fluoride). It is well known that PVF has good UV resistance and enhances module service life. Backsheet with aluminum film has low WVTR (water vapor transmission rate) value. Low WVTR module is helpful in guarding against water penetration into module, increasing module service life, according to ASTM F1249 standard test method for water vapor transmission rate through plastic film and sheeting using a modulated infrared sensor. Figure 2.1.4.5 shows the WVTR testing results.
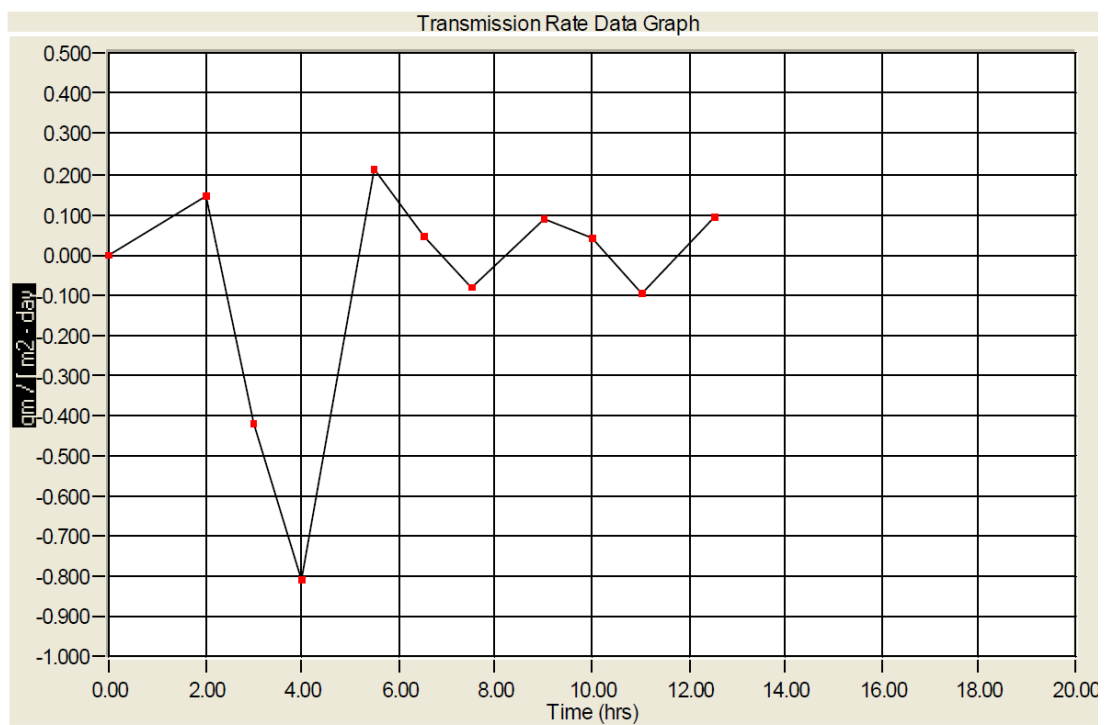
TEST RESULTS	IN SELECTED UNITS		IN STANDARD UNITS	
Transmission @ 97.0%	0.091254	gm / [m2 - day]		
Transmission @ 90.0%	0.084649	gm / [m2 - day]		
Permeation:	9.837150	gm - µm / [m2 - day]	0.387289	gm - mil / [m2 - day]

Figure 2.1.4.5 Aging module WVTR testing results

The WVTR testing of aging Penghu module showed that the module had only 0.091 gm/m^2-day, about 97.0% penetration. The typical number for commercial module is below 2 gm/m^2-day. It is clear that the WVTR performance of the aging

module is better than that of existing modules.

2.1.5 Aluminum frame analysis

Aluminum frame is the main structural strength of the module. Aluminum frame, therefore, needs to be strong enough to "fix" a given module and withstand typhoon and earthquake for 25 years. Aluminum frame generally use 6000 series aluminum alloy, i.e. magnesium silicon aluminum alloy. According the element ratio, there are 6061, 6063, 6066 types. The aluminum frame for the PV system mainly uses 6063 aluminum alloy, which has excellent mechanical properties, weldability, and processability. Annealing and heat treatment affect the mechanical properties of aluminum alloy. According the different annealing degree, the mechanical strength of aluminum alloy can be divvied to T0, T1, T4, T5, T6 types. T0 type aluminum alloy without annealing shows excellent ductility and poorer mechanical properties. T4 type aluminum alloy shows better ductility and lower mechanical properties. T6 type aluminum alloy shows poorest ductility and best mechanical properties. The mechanical properties of T5 type aluminum alloy is between that of T4 and T6. T4, T5, and T6 are commonly used aluminum alloy for PV system. Oxidized aluminum is a good protection layer for better mechanical properties, wear resistance, and anti-oxidation. The oxidized aluminum frame therefore is used for PV system, which is operated in the outside environment.
The analysis results of the aging aluminum frame show:

2.1.5.1 Assembling the aging aluminum frame

The 10–175 W modules are middle/small size modules produced before 2004. Typically, the module was assembled/screwed by hand. Due to the need of bigger modules in the PV market, manufacturers were able to produce 180–310 W modules starting at the beginning of 2005. The assembling of long and short aluminum frame is replaced by L-type key to avoid low quality hand screwing process. The aging module was produced by hand screwing. There are no defects, such as stripping or decomposition. It is evidence that the quality of the module is very good even after 17 years in operation. Figure 2.1.5.1.1 shows the assembled out-looking of the aging module.

Figure 2.1.5.1.1 Aging module is assembled by screw

Figure 2.1.5.1.2 currently use L-type key assemble elements

2.1.5.2 The Anode treatment of aluminum frame

Since aluminum is a very active metal, the anode treatment offers a good oxidized film, which offers a good layer with good mechanical properties, wear

resistance, and anti-oxidation for 25 years of operation. QuaNix 4500P (Non -
destructive film thickness meter) was used to measure the film thickness according to
DIN 50981/50984, BS 5411(3, 11)/3900(C, 5), ISO2178/2360/2808, ASTM B499/D
1400 standard. It is the fastest way to measure the thickness of anode treatment film.
Table 2.1.5.2.1 shows the anode treatment thickness of current commercial and aging
aluminum frame.

Company Name of aluminum frame	Thickness of anode treatment (μm)					Average thickness (μm)
Aging (Kyocera)	16.2	16.4	17.1	18.0	18.5	17.2
B	16.9	17	17.1	17.1	17.3	17.1
C	12.2	12.3	12.4	12.5	12.6	12.4
D	13.9	14.1	14.1	14.2	14.2	14.1
E	12.9	13	13	13.1	13.2	13

Table 2.1.5.2.1 Anode treatment thickness of current commercial and aging aluminum frames

2.1.5.3 Potential corrosion of aluminum frame

The aging Penghu PV system, built in 1999, was maintained in 2007. When the
module was fixed on the system supporting structure, insulating plastic gasket ring was
placed between aluminum frame and system supporting structure sue to potential
corrosion consideration. The gasket ring prevented electricity conductivity between
stainless screws and aluminum frame. Conductivity results in potential corrosion
phenomenon. After analyzing the aging PV module, it is found that all 20 modules'
screw positions show potential corrosion. Some assemble holes even had completely
collapsed. It is concluded that the whole aluminum frame go through anode treatment
before re-assembling. During re-assembling, the frames were drilled then screwed. The
drilled holes without anode treatment results in potential corrosion although gasket
rings were used. It is believed that the salt in the air accumulated inside the holes,
forming electric conductivity, and resulted in potential corrosion.

Figure 2.1.5.3.1 Potential corrosion of aluminum frame

2.1.6 Glass analysis

Typically, PV modules use low iron and light transmission tempered glass. The thickness of glass depends on the structure design. Light transmission affects the efficiency of PV module. Since iron content in glass results in green color of glass, PV module therefore use low iron glass. Glass not only offers module strength but also offers protection and wear-resistance. The glass on the aging module did not show any broken phenomena. There is only one module that fell to the ground due to corrosion of the aluminum frame. It is no related to the strength of glass. It is concluded that the strength of the glass used in the aging modules met the requisitions. The thickness of aging module is 3.2 mm. Figure 2.1.6.1 shows that the light transmission of the glass is only 81%, after having operated in Penghu. The typical light transmission of commercial anti-reflective glass, used in the PV module, is above 91%.
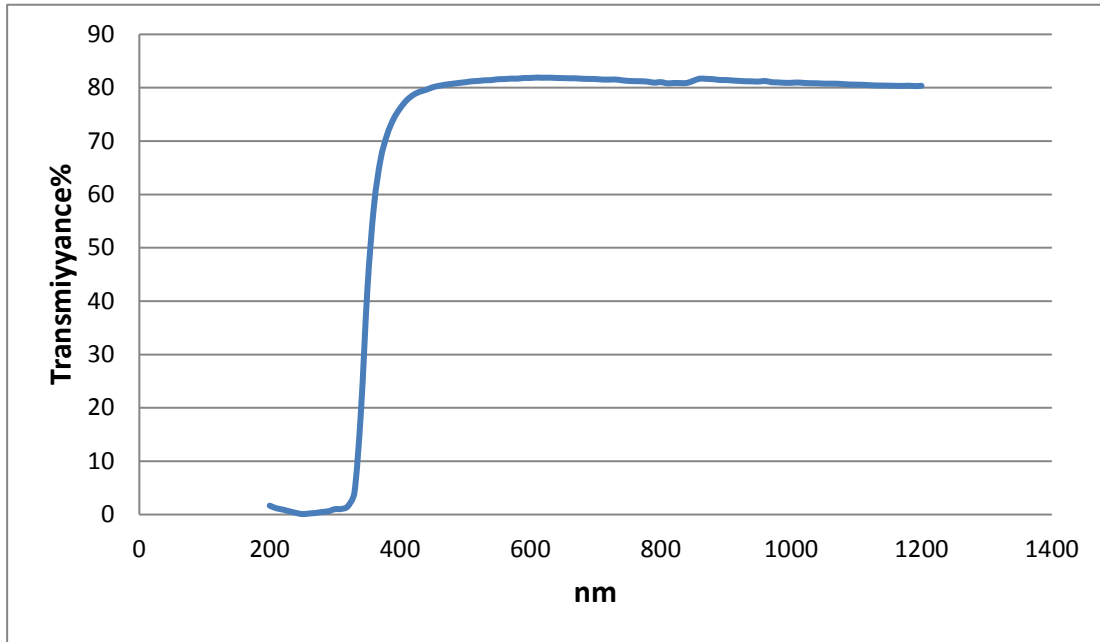
Figure 2.1.6.1 light transmission of aging glass

2.1.7 Junction box analysis

The structure and materials in the aging junction boxes are in good conditions after 17 years operation in the harsh environment. Polymeric materials were used to fill in the junction box. It is beneficial to guard against high humidity and high salt environment operation, keeping metal conductivity elements from corrosion. Figure 2.1.7.1 shows the diode and polymeric materials status inside the box. Figures 2.1.7.2 and 2.1.7.3 show the FTIR analysis of the polymeric materials. After Library search, the material is dimethyl siloxane. It is a silicon rubber type material with hard and brittle properties. Since the rubber is in good status, it is suspected that thermal conductivity materials were added into the rubber. The main failure mode for the aging junction boxes is diode burn out/peel off. It is suspected that the soldering point of ribbon was not treated very well. The local high temperature results in diode burn out/peel off because two of three burn out/peel off diodes were located at the edge of the box, near the soldering point of ribbon. The statistic of diodes status is listed in table 2.1.7.1. Figure 2.1.7.4 shows FTIR analysis and after Library search to find the material of the cover of junction box. It is confirmed that the material is PPO type materials. Figure 2.1.7.5 shows FTIR analysis and after Library search to find the material of the cover of cable connector. It is confirmed that the material is polyamide type materials.

Figure 2.1.7.1 Diode and polymeric materials status inside the box
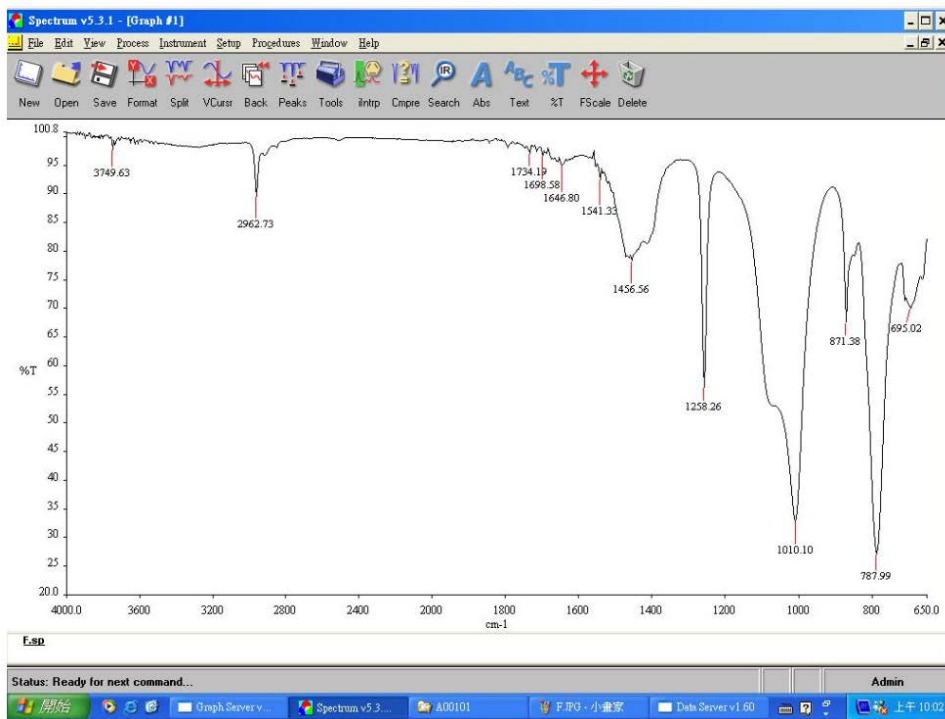
Figure 2.1.7.2 FTIR analysis the polymeric materials
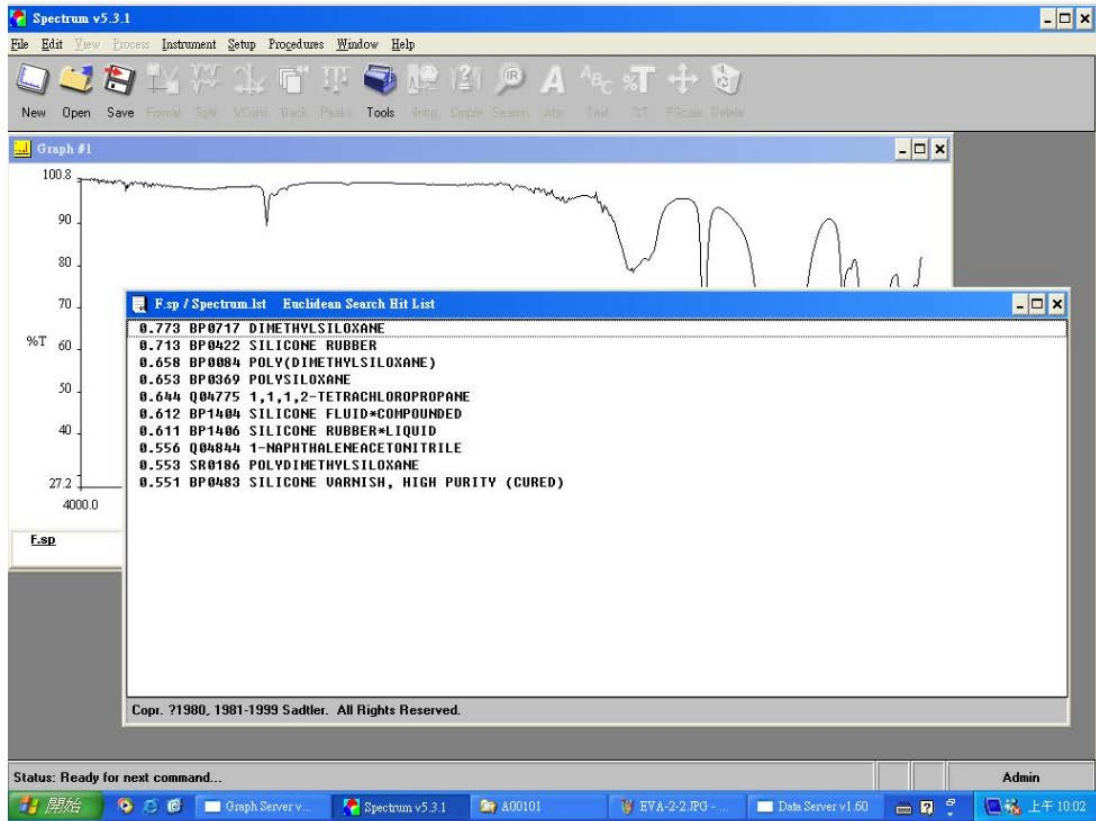
Figure 2.1.7.3 FTIR analysis of the polymeric materials through Library search
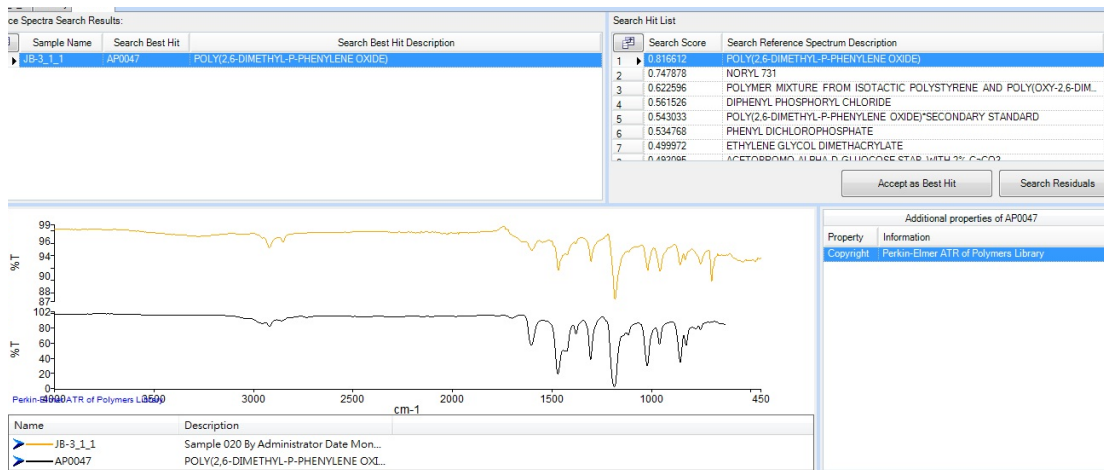
Figure 2.1.7.4 FTIR analysis and Library search to find the material of the cover of the junction box
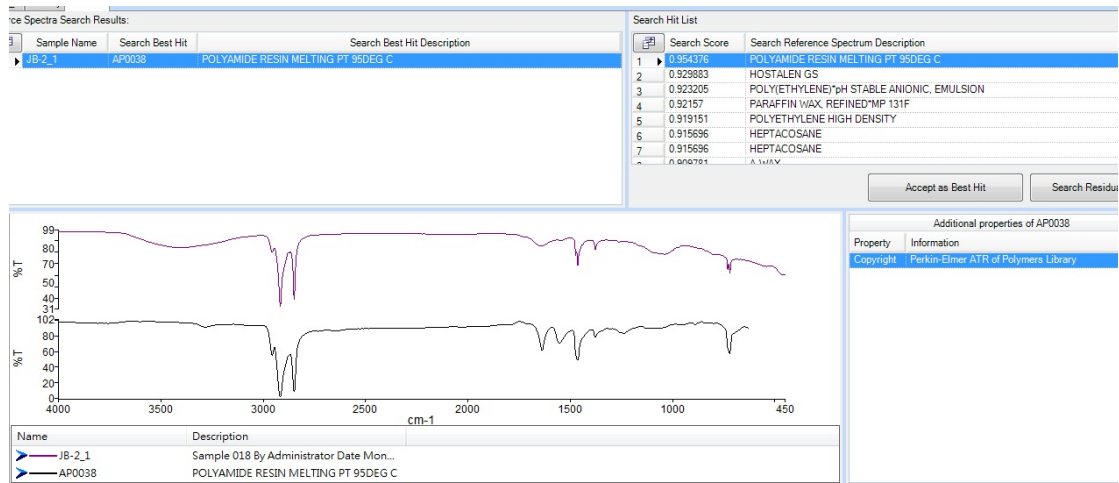
Figure 2.1.7.5 FTIR analysis and Library search to find the material of the cover of cable connector

Module Number	Pmax (W)	Diode status	Remarks
A2	65.51	Burned out	*1
A3	107.91	Good	*1
A4	117.76	Good	*1
A5	63.19	Burned out	
A6	114.44	Good	*1
A7	103.62	Good	
A8	0.00	Burned out	
A9	118.17	Burned out	*1
A10	67.86	Good	
B1	62.43	Burned out	*1
B2	0.00	Good	
B3	3.62	Burned out	
B4	0.00	Burned out	
B5	17.60	Burned out	
B6	63.97	Burned out	*1
B7	65.49	Burned out	

B8	67.49	Burned out	
B9	111.12	Good	*1
B10	118.10	Good	*1
B11	55.92	Burned out	*1

Table 2.1.7.1 Diode status of aging modules

*1: After re-building the module, the module is installed back to the PV system for data tracing

2.2 Specifications of the key components

Since Chinese Taipei is located at high temperature and humidity environment, which results in corrosion of PV module, the corrosion problems need to be addressed to promote PV system installation. To enhance the PV module service life and confront the PV module degradation caused by the harsh environment, backsheet and encapsulant play key roles. Having better water blocking property of backsheet and having encapsulant effectively inhibit moisture permeation and metal ion migration, both slow down corrosion, resulting in longer service life of the PV module. Improvement of PV module reliability can be through enhancing the key elements' properties, such as electric volume resistivity, coefficient of water absorption, water vapor transmission rate (WVTR), and voltage endurance.

EVA polymeric insulation material needs enough insulation resistance properties, which is decided by its electric volume resistivity. Agilent 4339B high resistance meter is used to test the DC resistance and electric conductivity properties of insulation material according to ASTM D 257-07. The test sample is applied 500 ± 5 V for 60 seconds to measure the change of its electric volume resistivity. If the electric volume resistivity is higher than $1014\Omega \cdot cm$ in high temperature and humidity environment, it means that the commercially available EVA encapsulant passes the minimum threshold of need.

The changing coefficient of water absorption of EVA encapsulant under high temperature and humidity (85°C/85% RH) is executed following ASTM (D570–98) standard test method for water absorption of plastics (chapter 7.1Twenty-Four Hour Immersion). The EVA's coefficient of water absorption should be ≤0.1% under the mentioned environment. The criterion is to ensure that a given EVA has the capability to slow down corrosion and prevent potential failure of the module.

Since backsheet is a water vapor barrier, the moisture-barrier properties also should be addressed. Water vapor transmission rate is selected to evaluate the

properties under ASTM F1249. Certainly, the thickness of backsheet affects its water vapor transmission rate, which needs to be far below 2 g/m^2-day.

Whenever the module is operated in a given PV system, the module needs to not only withstand rated working voltage, but also short-term over-voltage, which is higher than rated working voltage. The internal structure of EVA will change during over-voltage action. When the over-voltage strength reaches a certain value, the insulation material will become a conductor, resulting in sudden insulation breakdown. The phenomenon is called electric breakdown. If electric breakdown happens between electrodes, the phenomenon is called breakdown, which results in module electric leakage. The phenomenon is especially important when the module is operated in high temperature and humidity environment. The property of the module, therefore, needs be further evaluated under ASTM D149. In general, the breakdown voltage of commercially available aged EVA is over 20 KV, which is the minimum or basic requirement for insulation materials.

The aluminum frame of modules stands corrosion in highly corrosive environment after anode treatment. It is a very important treatment for the aluminum frame. Also the quality of the treatment is very important because the treatment will results in different degrees of corrosion from different aluminum frame suppliers. Micro-voids, pitting, can be seen on the surface of aluminum frame under scanning electron microscope (SEM). It is destructive for engineering structure, when pitting runs through the metal.

After testing the commercially available EVA and Backsheet and the mentioned module anti-corrosion methods, specifications can be set up for high temperature and humidity environment. The new specifications are:

For EVA: electric volume resistivity >1014 Ω•cm, coefficient of water absorption <0.1%, breakdown voltage >20 kV

For backsheet: WVTR value <2 g/m2-day

These specifications enhance the reliability and anti-corrosion capability under high temperature and humidity environment. The related specifications are list in table 2.2.1.

Parts Name	Test items	Specifications	Remark
EVA	Electric volume resistivity		ASTM D 257-07
EVA	Coefficient of water absorption	<0.1%	ASTM D570-98
EVA	Breakdown voltage	>20 kV	ASTM D149
Backsheet	Water Vapor Transmission Rate (WVTR)	<2 g/m^2-day	ASTM F1249
Aluminum frame	Thickness of anode treatment	≥12 µm	

Table 2.2.1 The specifications of key parts for enhanced reliability and anti-corrosion capability

3 The original, maintained/reconstructed PV system, at Penghu County Government

3.1 Modules maintenance of the original PV system

3.1.1 Maintenance of ribbon connection and backsheet

The wider ribbon connection is not in good contact condition, due to the wider ribbon connection without applying tin-lead alloy to protect/strengthen the contact. The poorer contact results in arcing, which creates high temperature in the contact. The contact high temperature results in the delaminated and bubble phenomena between backsheet and EVA. It is found that some modules had only 50% module power left. The worst one or two modules do not have power output. The modules therefore needed maintenance. The maintenance procedures were:

- Cut off the delaminated backsheet and EVA
- Applying tin-lead alloy to strengthen the connection of wider ribbon-completed connection
- Laminate new EVA and backsheet (figure 3.1.1.1)
- Trim off redundant EVA and backsheet at module edge and install new junction box
- If the restructuring module passes IEC61215ed.2 wet leakage current test, the modules are qualified to be used.
- Power test needs to be above 80% of the original specification
- Install new aluminum frame

Figure 3.1.1.1 Laminate new EVA and Backsheet and install new junction box

3.1.2 Maintenance of the aluminum frame

All aluminum frames were replaced, due to serious potential corrosion. Otherwise, the poor mechanical load of the modules cannot withstand gale and typhoon. All aluminum frames were drilled needed holes, before anode treatment. The procedures made sure that the frames will not have potential corrosion issues. It should be addressed that the aluminum frame must form a continuous electric path. Otherwise, the finished module will not pass EC61730-2 MST13 ground continuity test. Figure 3.1.3.2 shows the before/after maintenance of the original modules.
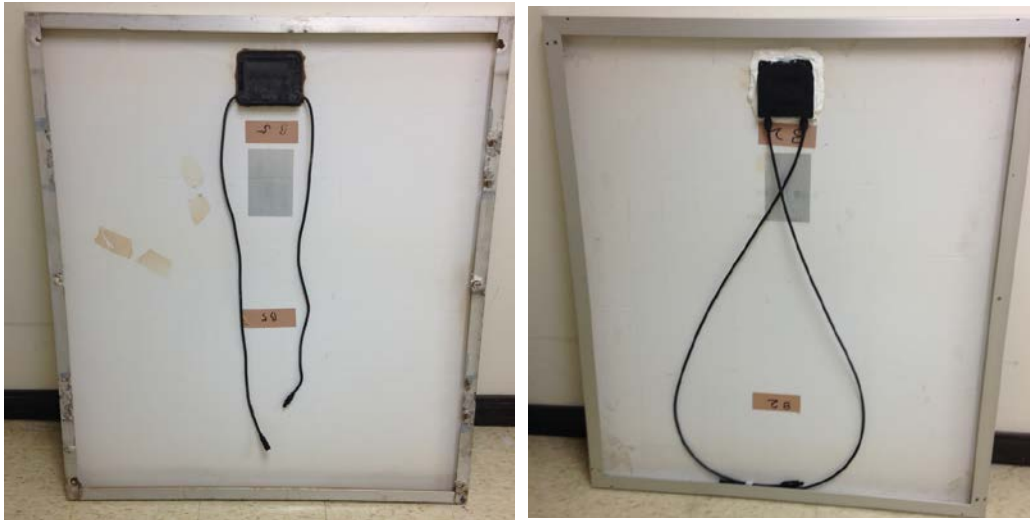
Figure 3.1.2.1 Maintenance of the original module

Left: before maintenance; right: after maintenance

3.1.3 The replacement of junction box and connector

Tyco junction boxes were used to replace the existing junction boxes because diodes were burned out after long periods of operation in the harsh environment. Also, the metal elements inside the junction box's connector showed atmospheric corrosion. Since connectors connect modules, the electric properties needed to match each other. For these two reasons, the junction box had to be replaced by new Tyco junction boxes.

Figure 3.1.2.1 Junction box replacement

Left: before replacement; right: after replacement

Figure 3.1.2.1 The connector replacement

Left: before replacement; right: after replacement

3.2 Modules restructuring of the original PV system

Since the system had been in operation for 17 years, the degree of decay of the module's output voltage/current/power is different and far from the original electric properties. Eleven modules with higher/better electric performance (after maintenance) were selected to design a module array. The array was installed back to the original place to study the system performance after the mentioned maintenance. Preliminary data shows that the system reached 80–90% of the rated power. One module array with brand new module was installed at the same place. The new array was designed to be six by seven cells. The comparison between maintained and new array was carried out to know the different power generating capacity between two arrays.

Module No.	Voc (V)	Isc (A)	Vmp (V)	Imp (A)	Pmax (W)	FF (%)	% of rated power	Remark
A2	25.13	6.94	19.16	6.35	121.61	69.72	90.08%	*
A3	24.69	6.91	18.63	5.95	110.79	64.93	82.07%	
A4	25.04	6.95	18.75	6.34	118.88	68.33	88.06%	
A5	25.05	6.98	20.48	5.68	116.30	66.57	86.15%	*
A6	24.80	6.97	18.68	6.40	119.48	69.10	88.50%	
B1	24.67	6.87	19.14	6.08	116.46	68.71	86.27%	
B6	24.88	6.91	19.11	6.34	121.16	70.49	89.75%	*
B7	24.89	6.99	19.18	6.37	122.49	70.39	90.73%	
B9	26.12	7.05	17.82	6.21	110.61	62.60	81.93%	
B10	24.81	6.86	19.07	6.28	119.74	70.32	88.69%	
B11	24.71	6.88	17.95	6.14	110.23	64.82	81.65%	

Table 3.2.1 Power test data of maintained modules

*: welding repair between wider ribbon and long strip EVA & backsheet was used to

strengthen the insulation of module

Module No.	Module area (m^2)	Wet leakage current (MΩ)	Wet leakage current (MΩ).m^2	Requested specification (MΩ).m^2	Judgement
A2	1.084	177.2	192.08	40	qualified
A3	1.084	172.1	186.56	40	qualified
A4	1.084	235.0	254.74	40	qualified
A5	1.084	167.3	181.35	40	qualified
A6	1.084	167.0	181.03	40	qualified
B1	1.084	190.4	206.39	40	qualified
B6	1.084	248.0	268.83	40	qualified
B7	1.084	221.3	239.89	40	qualified
B9	1.084	243.0	263.41	40	qualified
B10	1.084	191.4	207.48	40	qualified
B11	1.084	177.0	191.87	40	qualified

Table 3.2.2 Wet leakage current test of maintained modules

Module No.	Out looking (status)	Junction box	Connector	Aluminum frame
A2	*A (good after repair)	replace	replace	replace
A3	*B (usable)	N/A	replace	replace
A4	*C (usable)	N/A	replace	replace
A5	*A (good after repair)	replace	replace	replace
A6	*C (usable)	N/A	replace	replace
B1	*C (serious)	replace	replace	replace
B6	*D (usable)	replace	replace	replace
B7	*A (good after repair)	replace	replace	replace
B9	*C (serious)	N/A	replace	replace
B10	*B (usable)	N/A	replace	replace
B11	*B (usable)	replace	replace	replace

Table 3.2.3 the status of original module and maintenance conditions

*A: welding repair between wider ribbon and long strip EVA & Backsheet was used to strengthen the insulation of the module

*B: Backsheet defect(s) at module corners

*C: Backsheet defect(s) at module upper corners

*D: Aluminum foil of backsheet was oxidized

Parts name	Brand	Model/Specifications
CELL	Mosel Vitelic Inc.	6" Poly MBX-25 200±20 μm 17.4% 4.234~4.283W BB (3 Bus)
String connector	Banner International Corp.(Misuzu)	0.2 mm*1.6 mm (width:1.6 mm) TPB
Busbar connector	Solarjoin Technology Inc.	0.3*5.0 mm Sn 60% Pb 40%
EVA	3M	9110T high-penetration 0.45 mm + 9120B high volume resistant 0.45 mm
Backsheet	Coveme	PYE P50/P125/EW 295u
Glass	Xinyi Glass Holdings Limited	Tempered 1310*990*3.2 mm Texture
Junction box	Tyco	4 rails 3 diode TYCO-1971482-2 L:120 cm
Adhesive (silicone)	Momentive	TSE-382
Frame	Chida Aluminum Incorporation	40 mm frame thick:1.5 mm *A

Table 3.2.4 Specifications of module parts for the new module array

*A: electric ground symbol, processed before anode treatment

Module No.	Voc (V)	Isc (A)	Vmp (V)	Imp (A)	Pmax (W)	FF (%)
CJH00468	26.40	8.80	21.12	8.26	174.49	76.10
CJH00470	26.39	8.79	21.18	8.24	174.50	76.28
CJH00471	26.40	8.83	21.14	8.27	174.67	74.94
CJH00472	26.38	8.84	21.12	8.27	174.41	74.80
CJH00473	26.40	8.80	21.12	8.26	174.32	75.04
CJH00474	26.39	8.86	21.12	8.25	174.15	74.47
CJH00475	26.35	8.78	21.14	8.26	174.38	75.42
CJH00477	26.37	8.82	21.11	8.25	174.13	74.83

CJH00478	26.35	8.81	21.13	8.24	174.05	75.03
CJH00479	26.35	8.86	21.07	8.26	173.94	74.67
CJH00480	26.37	8.86	21.08	8.25	173.96	74.44

Table 3.2.5 Power test data of brand new modules

Module No.	Module area (m^2)	Wet leakage current (MΩ)	Wet leakage current (MΩ).m^2	Requested specification (MΩ).m^2	Judgement
CJH00468	1.309	7868	10299	40	qualified
CJH00470	1.309	7383	9664	40	qualified
CJH00471	1.309	7945	10400	40	qualified
CJH00472	1.309	>9999	>13089	40	qualified
CJH00473	1.309	8044	10530	40	qualified
CJH00474	1.309	6159	8062	40	qualified
CJH00475	1.309	8487	11109	40	qualified
CJH00477	1.309	9889	12944	40	qualified
CJH00478	1.309	>9999	>13089	40	qualified
CJH00479	1.309	>9999	>13089	40	qualified
CJH00480	1.309	7537	9866	40	qualified

Table 3.2.6 Wet leakage current test of brand new modules

4 The PV system

4.1 The Design of the Penghu PV system

The Penghu PV system is one of the Green Energy Photovoltaic Demonstration Research Systems. The system was installed in Penghu to study the long-term influence for a given PV system in harsh, high salt, high humidity environment with monsoon on an outlying island. The PV system was installed on the third floor of the Construction Bureau of Penghu County Government in June 1999. The total area of the solar array is 23.32 square meter. The system's parts were maintained/replaced in December 2007 to resume power output. Modules had been in use continuously. The specification of the system is listed in Table1.3.1.

The maintained parts were mainly PV system bracket, DC cable confluence groove and disk maintain, AC switchboard, monitor box, and inverters, etc. The system resumed power output and on grid in 2008. Figure1.3.3 shows the monitor display of the Penghu PV system. DC combiner box was installed on the side of array bracket. AC power panel, inverter, and watt hour meter were installed. AC power panel, inverter, monitoring system, transformer, and watt hour meter, were installed on the first floor wall of the Civil Engineering department. After the large scale maintenance in 2007, the parts were used for more than 8 years. The status of the parts warrant further researching.

Figure 4.1.1 The monitor display of the Penghu PV system

The PV system was inspected in 2016. The system was not connected to the city

power system due to parts malfunction. During long-term monitoring of the system, it is found that inverter with shortest service life was about 3–5 years. Other malfunctioned parts were:

1. The cable connection points inside monitor display with corrosive phenomena. The LED display did not function.

2. AC/DC power panel was protected by the monitor box. The parts were still working and could be used.

3. Inverter was not working. The paint on the inverter surface had corroded. Cooling fan was stuck and could not rotate. The cable still could be used. The soldering point and connector of PCB showed aging phenomena. Figure 4.1.1–3 show all the mentioned phenomena.

Figure 4.1.2 AC/DC power panel and inverter of the Penghu PV system

4. Because DC combiner box and DC combiner box were installed on the side of the rooftop array bracket, the connector of cable, which was near the interface of inner and outside monitor box, started corroding under harsh environment. The monitor box had fallen down because the corrosion of the screws, which were used to fixed the box. Rain, therefore, enter the monitor box and the damaged the parts.
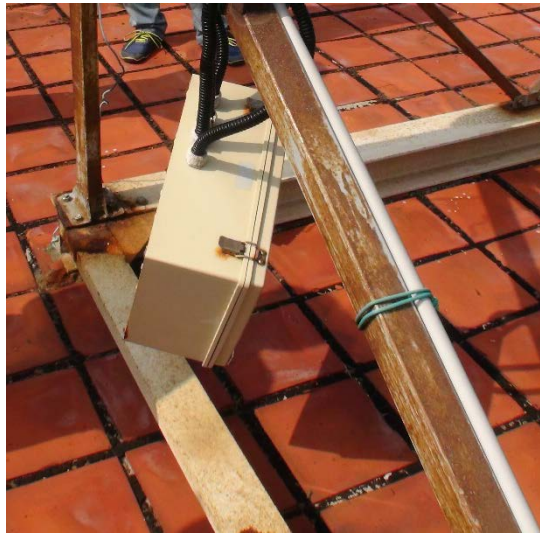
Figure 4.1.3 Monitor box fallen down

Figure 4.1.4 The monitor box

5.   The PV system is designed for harsh environment, high salt, high humidity, and monsoon, to be placed on outlying islands in June 1999. The base of bracket used H shape stainless. Screw ground anchor was used to fix the bracket and rooftop floor. The whole bracket used stainless. Aluminum trays were used as the cable pathway. Bracket and the base of the bracket was painted to prevent corrosion. After years of operation, the H shape stainless was under good condition. Small area of corrosion was found at the connecting point with other materials. The corrosive phenomenon was not expected to damage the damage of the structure. Figure 4.1.5 shows the

mentioned corrosive phenomena. Figure 4.1.6–7 show the contact point corrosion between bracket base, screw, nuts, and H shape stainless. Figures 4.1.8 and 4.1.9 show that the corrosive phenomena on the surface of bracket and soldering point of bracket respectively. The cover of DC cable tray was deformed and cannot be sealed completely. A lot of waterproof connector had fallen down or dismiss at the enter point of the cable tray. The surface of DC cable trays showed corrosion. The anti-UV cable, which were used in the Penghu PV system, had aging and cracking phenomena (Figure 4.1.11).

Figure 4.1.5 Corrosive phenomena on bracket

Figure 4.1.6 Status of screws and nuts

Figure 4.1.7 Contact point corrosion between bracket base, screws, nuts, and H shape stainless

Figure 4.1.8 Corrosive phenomena on the surface of bracket

Figure 4.1.9 Corrosive phenomena on soldering point of bracket

Figure 4.1.10 DC cable tray status

Figure 4.1.11 Anti-UV cable had aging and cracking phenomena

6. Some modules had fallen down during the summer typhoon season because of the corrosion of the module frame (Figure 4.1.12). The certified modules were moved back to Hsinchu laboratory for further examination to assess the status of the modules. The results were discussed in chapters 1 and 2.

Figure 4.1.12 fall down module

4.2 Failure mode of the PV system and improvement methods

The root cause for the Penghu PV system to have stopped working was corrosion, because the system operated long-term in harsh environment. As mentioned above, most modules can be repaired and resume their functions. Figure 4.2.1–2 show that grinder was used to remove the rust on the bracket and its base. All rust on the surface of stainless materials should be removed to extend the service life of the parts. After removing rust, anti-rust paint was painted on the surface (Figure 4.2.3). Figure 4.2.4 shows that the surface of metal/stainless was painted using traditional paint, after painting on anti-rust paint, to finish the maintenance process. After removing rust, painting anti-rust paint, and painting traditional paint, PV modules were put back to the bracket. Eleven brand new and repaired modules were installed on the maintained bracket. The brand new and repaired modules were installed at the upper and lower array in the system respectively. Figure 4.2.7 shows the new DC cable tray. The monitor system and inverters were replaced by new ones. The Penghu PV system performance after repaired will be discussed at the following sections.

Figure 4.2.1 H shape stainless and the base of bracket after removing rust

Figure 4.2.2 Stainless bracket after removing rust

Figure 4.2.3 Bracket base after painting anti-rust paint

Figure 4.2.4 Surface of metal/stainless after maintenance

Figure 4.2.5 Finished system bracket

Figure 4.2.6 Modules were installed back to the system bracket

Figure 4.2.7 New DC cable tray

4.3   The monitoring system of the PV system

4.3.1 PV monitor system design

The main elements and data for monitor system are:

Pyranometer:

DELTA OHM LP-PYRA03AC follows ISO 9060 Second Class

T-type thermocouple: measure module temperature, data are available from analog-to-digital converter

DC data: voltage, current, power, watt-hour

AC data: voltage, current, power, watt-hour, frequency, and power factor
Both DC and AC data taken from inverter communication

All above mentioned data were collected through data logger at time-cycle type sampling base. The "software control engine" was the core software to input/output the I/O control, measurement scheduling, command parser, and data distribution. The data was collected and recorded every ten second. Data logger showed the related data on the display of monitoring system through internet in real-time. Figure 4.3.1.1 shows the structure of the monitoring system. Figure 4.3.1.2 shows the DC box of the monitoring system. Figure 4.3.1.3 shows the AC box of the monitoring system. Figure 4.3.1.4 shows the real-time display picture of the monitoring system
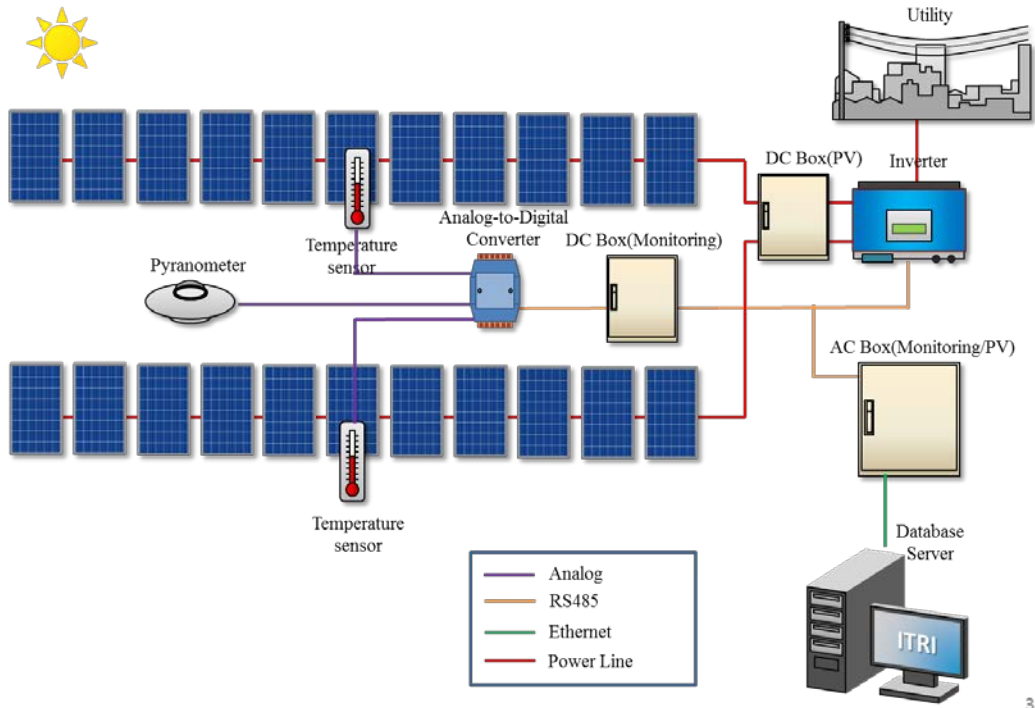
Figure 4.3.1.1 Structure of the monitoring system

Figure 4.3.1.2 DC box of the monitoring system

Figure 4.3.1.3 DC box of the monitoring system
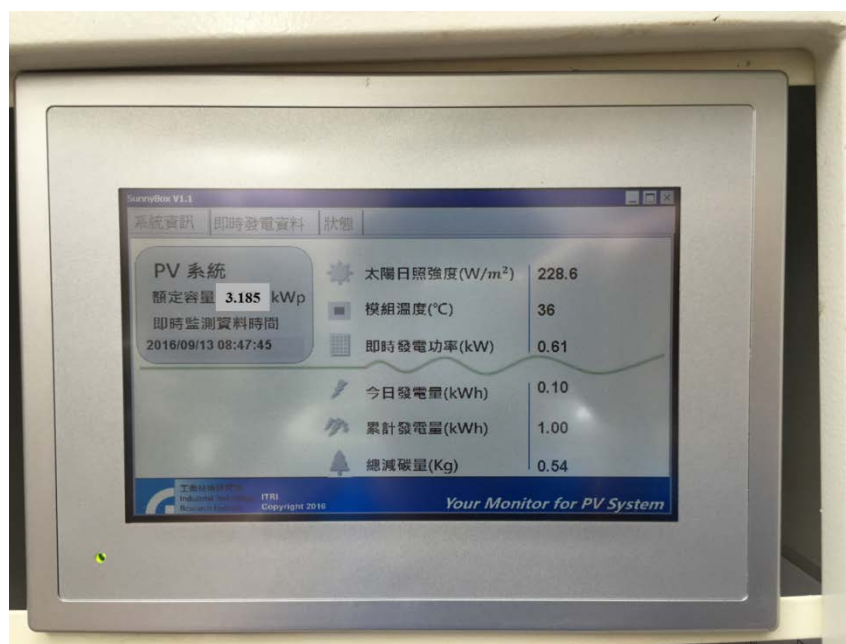
Figure 4.3.1.4 Real-time display picture of the monitoring system

4.3.2 Methods for PV system improvement

Since the aging PV system was installed in the high salt area, the parts of the

monitoring system and boxes should be strong enough, corrosion-resistant, have long service life, fast heat dissipation, maintenance-free, easy to clean, have smooth veneer, reasonably priced, and high weathering resistant and have high reliability. The outdoor box to be used especially need to have the following properties: anti-corrosion, anti-salt damage, and high air tightness. Aluminum alloy with anodized treatment is a good solution. Also, the chosen inverter needs the following specifications:

(1) The peak power tracking voltage range should fit in the output voltage of the designed PV system.

(2) Inverter should be compliant with relevant specifications and verifications, such as IEEE 1547, IEEE 929, UL 1741, VDE 0126-1-1, IEC 62109, etc. Certainly, the inverter needs to follow the safety rules of local power companies to be on grid.

(3) The rated output capacity needs to be confirmed and then choose suitable inverter to match the PV system.

(4) Power factor should be higher than 0.95. In general, higher power factor represent better output electric quality.

(5) The maximum efficiency of the inverter is higher than 92%. Higher efficiency represents better power generation efficiency.

(6) Whether the chosen inverter provide power generation data, capture function and the type of communication transmission mode, such as RS-485, RS-232.

(7) Total harmonic distortion should be in compliance with specifications, such as IEEE-519-1992, IEEE recommended practices and requirements for harmonic control in electrical power systems.

(8) For on grid PV system, inverter needs to meet the city power voltage requisitions. For off grid type PV system, inverter should be in compliance with

the voltage demand of AC load. It is recommended to avoid using transformers due to voltage differences. The output voltage frequency of inverter should be in compliance with local city power frequency. For example, 60 Hz is needed for the applying in the Chinese Taipei area.

4.4 Solar irradiation and power generating capacity data analysis

Generally speaking, there are two indices to evaluate the long-term performance of installed and operated PV systems. The evaluation period for a given PV system can be one day, one week, one month, or one year. It all depends on the need. The longer evaluation period can better represent the PV system's real performance. Two PV system performance evaluation indices are described below.

4.4.1 Solar irradiation calculation method

PSH (daily peak sun-hrs) can be used to evaluate ideal power generating capacity of a given PV system. For a rated capacity 5kWp PV system, the ideal daily power generation is 25kWh under five hours of sunshine per day.

$$PSH = \frac{H_I}{G_0}$$

H_I: solar radiation during evaluation period (kWh/m^2)
G_0: Standard sunlight intensity (1000 W/m^2)

4.4.2 Calculation methods for power generating capacity

Daily Mean Yield (DMY)

The calculation equation for DMY is listed below. The unit for DMY is kWh/d/kWp.

$$DMY = \frac{E_{out}/\text{day}}{P_o}$$

E~out:~: power generation under the evaluation period (kWh)

P~0~: the rated power of PV system (kWp)

Day: evaluation days

4.4.3 Recommendations for enhancing power generating capacity

Performance Ratio (PR)

Performance Ratio (PR) is an index to represent the real/ideal PV system performance. Basically, PR is not related to the position, tilt angle, azimuth angle, or rated capacity of a given PV system. The PR value is related to module tested power, module array shading, dust on the surface of module, module efficiency loss due to temperature, cable transmission loss, inverter efficiency, maximum power traceability of Inverter , PV system design, parts matching design, and weather, etc. PR, therefore, is a crucial index for the power generation capability of PV systems. For an on grid type PV system, the equation for PR calculation is:

$$PR = \frac{E_{out}/P_0}{H_I/G_0}$$

E~out~: power generation under the evaluation period (kWh)

P~0~: the rated power of PV system (kWp)

H~I~: solar radiation during evaluation period (kWh/m^2)

G~0~: Standard sunlight intensity ($1000\ W/m^2$)

In general, cable transmission loss and inverter loss totals to about 10%. PR, over 90% is hard to achieve. If PR value is abnormally high, accumulated sun irradiation intensity and accumulated power generation are two key factors to be reviewed. Analog-to-digital converters malfunction and the surface dirty/shading of pyrometer are possible root causes. If PR value is abnormally low, module array shading, module array surface dirty, and inverter malfunction are possible root causes.

4.4.4 Data from re-constructed aging PV system

As mentioned previously, the PV system was installed on the third floor of the Construction Bureau of Penghu County Government in June 1999. The total area of the solar array is 23.32 square meter. The system can be grid-connected or off-grid, which offers 1.5 kilowatt AC (alternating current) electric power during day time. DC combiner box was installed at the array tripod corner. AC power panel, inverter, monitoring system, transformer, and watt hour meter were installed on the first floor wall of the Civil Engineering Department. After the mentioned reconstruction of the system, the reconstructed PV system operated and collected power generation related data from September 16 to December 31, 2016. The data are listed in tables below.

Monitored PV system capacity (kWp)	Sep.	Oct.	Nov.	Dec.
3.185	30	31	20	17

Table 4.4.4.1 Sampling days per month (Penghu Island)

Monitored PV system capacity (kWp)	Sep.	Oct.	Nov.	Dec.
3.185	4.71	4.44	4.36	3.55

Table 4.4.4.2 Cumulative Peak Sun-Hours per day (Penghu Island)

Monitored PV system capacity (kWp)	Sep.	Oct.	Nov.	Dec.
3.185	3.79	3.38	3.35	2.74

Table 4.4.4.3 Daily average power generation per month (Penghu Island)

Monitored PV system capacity (kWp)	Sep.	Oct.	Nov.	Dec.
3.185	80%	76%	77%	77%

Table 4.4.4.4 Performance ratio per month (Penghu Island)

Real-time power generation:

Date: October 24, 2016

Time: 11:59 AM

Sun irradiation intensity: 786.40 W/m^2

Module temperature: -1:49.09°C

Module temperature: -2:49.4°C

Data for DC	Voltage (V)	Current (A)	Power (W)
DC-1	206.30	5.50	1135
DC-2	186.70	4.06	758

Data for AC	Voltage (V)	Current (A)	Power (W)	Frequency (Hz)	Watt Hour (kWh)
AC-1	236.2	6.6	1783	59.99	381.8

Note:

-1: brand new PV system, which was installed in the same frame as the aging PV system

-2: reconstructed aging PV system

It is found that the PV system had no power output during times with bad weather of high humidity. Inverter shows the error message "Fast Earth Current Fault". It is suspected that the module leaked current or poor cable connection during soldering processes resulted in humidity penetration. The phenomenon needs to be further studied and repaired.

4.5 Comparison of the power output of similar PV System

4.5.1 Specifications of similar PV System

For comparison purpose, Chiayi High School PV system is identified from all monitored PV system in Chinese Taipei because the system had several similarities with the aging PV system, such as latitude, longitude, and rated PV system capacity. Table 4.5.1.1 shows the baseline information of the Chiayi High School PV system.

Monitored PV system capacity (kWp)	Installation date	Azimuth angle (degree)	Tile angle (degree)	Module type	Inverter type
3.69	Sep. 2009	south	18	Tynsolar TYN-220P6	Ablerex ES2200

Table 4.5.1.1 Baseline information of the Chiayi High School PV system

4.5.2 Comparison between the two systems' power generating performance

The DMY, PSH, and PR data of the Chiayi High School PV system is listed below. Data collection occurred from September 16 to December 31, 2016.

Monitored PV system capacity (kWp)	Sep.	Oct.	Nov.	Dec.
3.69	30	31	30	15

Table 4.5.2.1 Sampling days per month (Chiayi High School)

Monitored PV system capacity (kWp)	Sep.	Oct.	Nov.	Dec.
3.69	3.84	3.93	3.51	4.29

Table 4.5.2.2 Cumulative Peak Sun-Hours per day (Chiayi High School)

Monitored PV system capacity (kWp)	Sep.	Oct.	Nov.	Dec.
3.69	3.01	2.99	2.65	3.23

Table 4.5.2.3 Daily average power generation per month (Chiayi High School)

Monitored PV system capacity (kWp)	Sep.	Oct.	Nov.	Dec.
3.69	78%	76%	76%	75%

Table 4.5.2.4 Performance ratio per month (Chiayi High School)

Real-time power generation:

Date: October 24, 2016

Time: 11:59 AM

Sun irradiation intensity: 554.25 W/m^2

Module temperature: 66.76°C

Data for DC	Voltage (V)	Current (A)	Power (W)
DC-1	216.40	4.49	971
DC-2	218.20	4.21	918

Note: DC-1 and DC-2 are PV Input Power 1 and PV Input Power 2, respectively

Data for AC	Voltage (V)	Current (A)	Power (W)	Frequency (Hz)	Watt Hour (kWh)
AC-1	223.05	8.00	1771.91	59.98	14979.23
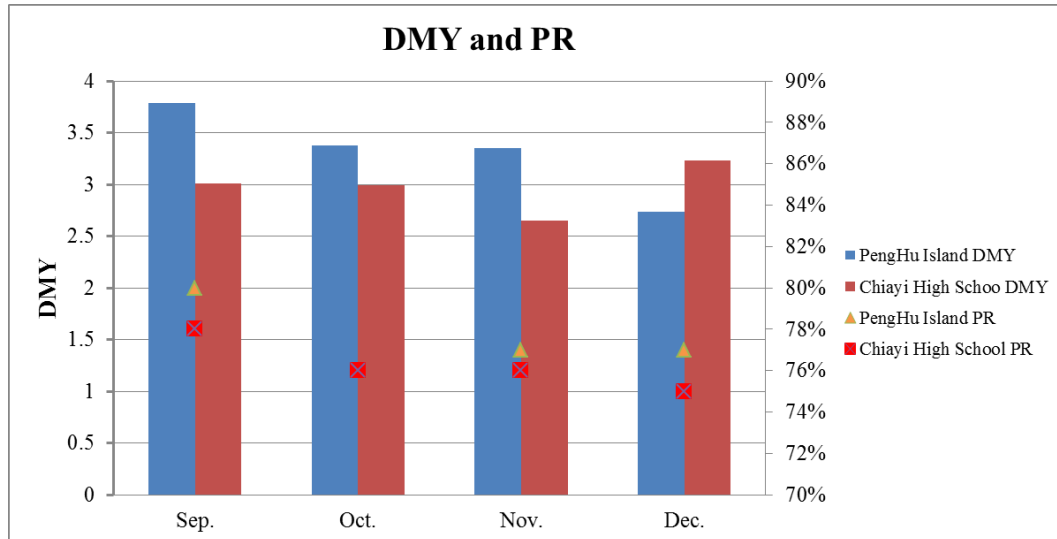
Figure 4.5.2.1 System index comparison between Chiayi High School and Penghu PV systems

Table 4.5.2.5 is the DMY comparison between brand new and repaired modules. The data were collected on October 24, 2016 under PSH 5.69. It is clear that the repaired modules' performance is slightly lower than that of brand new modules.

Data of DC	DMY	PR (%)
DC-1	5.11	90
DC-2	4.97	87

Table 4.5.2.5 DMY comparison between brand new and repaired modules

DC-1: brand new PV system, which is installed in the same frame as the aging PV system

DC-2: reconstructed aging PV system

5 Gender

5.1 Training program for banking mechanism for PV industry

The starting reason for PO self-fund "PV Promotion Project"

Chinese Taipei imports 98% of needed energy. Under the premise of global warming and the scarcity of natural resources, balancing economic development and enhanced energy independence is an urgent priority for Chinese Taipei. Chinese

Taipei is located in the subtropical zone, which is suitable for the development of photovoltaic and wind power. Since renewable energy does not demand fuel, it is only not susceptible to the fluctuations of international fossil energy prices, but also will not produce carbon emissions in the application process. It is, therefore, very helpful in improving environmental quality. Chinese Taipei triggered and aggressively deployed the PV promoting project in February 1991. An office was set up to plan and co-ordinate the relevant resources in the same year. A single administration window was set up to offer professional assistance to resolve obstacles, making the installation of PV more popular, and accelerated the related promotion goal. In line with Chinese Taipei's future electricity demand and low-carbon society target, the cumulative PV installation goal is 20GW. It is expected that the annual PV power output will reach 25 billion Kwh, reducing about 1305 million metric tons of carbon dioxide emissions, which is equal to planting 108.7 million trees.

The Training:

One of the crucial elements for promoting PV industry is the bankability for a given PV system. The financial suppliers, such as commercial bank, leasing companies, insurance companies, farmers' association bank, and venture capital, etc, need deeper understanding of risk management and control mechanisms for a given PV system. In order to provide related people with enough knowledge of PV systems, training was conducted by theChinese Taipei Academy of Banking and Finance Institute in July 2016. The training invited women to attend, in order to cultivate more females in the PV related supply chains. A total of 54 people (38 men and 16 women) attended the training. It is believed that the trained women will become pioneers in the PV bankability and supply chain. The trained women will also encourage more women to stepping into the PV financial related fields.

Figure 5.1.1 Overview of the training-1 Figure 5.1.2 Overview of the training-2

5.2 PV System Training

In view of the extreme weather anomalies in recent years, Chinese Taipei's various districts have suffered severe typhoons, resulting in serious damage to many PV systems and modules. This not only results in the loss of property, but also reduces the confidence in the solar photovoltaic system, consequently decreased the willingness of investors to invest. To enhance the quality, performance, safety, reliability, and durability of solar PV systems, a training symposium was organized mainly by the Industrial Technology Research Institute on November 24, 2016. The training was not only focused on the Solar Photovoltaic System Support frame structure design related research and exchange of research results, but also addressed the solar photovoltaic system acceptance, operation and maintenance issues, to share and look forward to strengthening the domestic solar photovoltaic system security, quality and reliability. There were 67 people who attended the training. Women were invited, and 7 attended the training. Figure 5.2.1–4 show the situation during the training.

Figure 5.2.1 Overview of the training-1

Figure 5.2.2 Overview of the training-2

Figure 5.2.3 Overview of the training-3

Figure 5.2.4 Overview of the training-4

5.3 Female laborers

As listed in the table 5.3.1, female laborers account for 50% of the total laborers. The short-term laborers from subcontractors cost about 60% of the total budget. Short-term laborers are purely female. In other words, the total laborer is much higher than 50%. From budget aspect, 80% of the budget is used to hire female laborers.

Name	Position/Role	Sex	Anticipated Time
Fu-Ming Lin	Division Director	male	0.5 month
Chen-Lung Huang	Project Manager	male	1 month
Chia-Wen Chang	Researcher	female	1 month
Yu-Hsuan Lin	Researcher	female	1 month
Mei-Hsiu Lin	Researcher	female	1 month
Wen-Haw Lu	Senior Researcher	male	0.5 month

Table 5.3.1 Labor distribution

6 Global PV trend

6.1 Solar PV module/ system cost analysis

In the first half of 2016, solar PV industry in China experienced the 630 installation rush. Imposed by the Chinese government, the 630 regulation allows solar power plants that completed installation before June 30, 2016 to sell electricity at a higher rate, and mandates that plants completed after July 1, 2016 to charge a lower rate. The installation capacity worldwide was estimated to reach 37GW during that period. Compared to the 26GW during the first half of 2015, installation capacity has increased by more than 42%. However, during the 3rd quarter of 2016, demand for solar modules dropped to less than 10GW due to the rapid cool-down of the world's largest market, China. As a result, product prices dropped drastically; module price decreased by nearly 20% during July and August.

According to Bloomberg New Energy Finance (BNEF) (Figure 6.1.1), installation cost for a ground-mounted large-scale (MW-scale) solar PV power plant was USD 1.31/W in 2015. It is estimated to drop to USD 0.97/W by 2020. Module price has dropped from USD 0.58/W to USD 0.37/W.
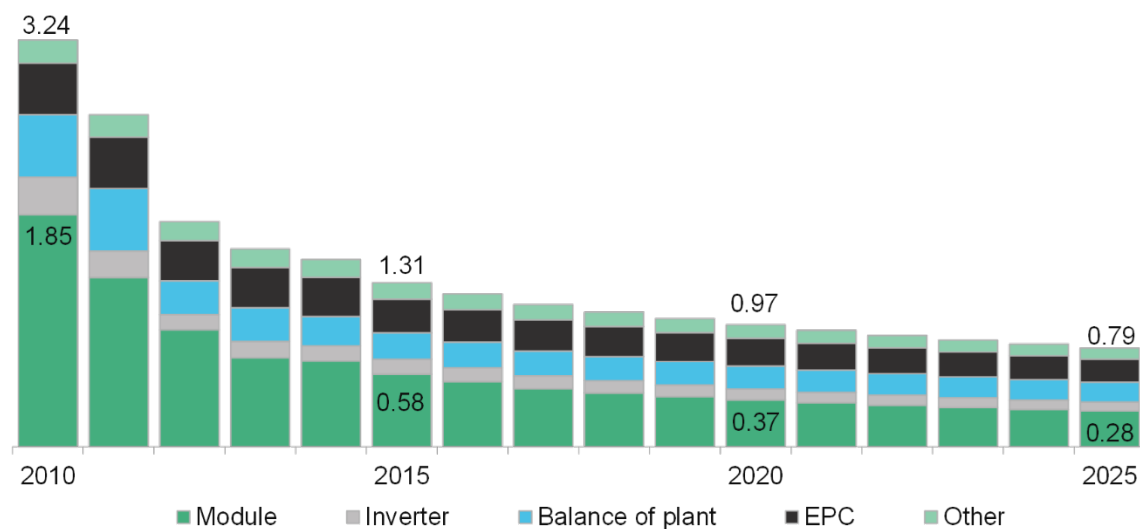
Figure 6.1.1 The cost for MW level power plan

By early September 2016, the price of solar module had come down to USD 0.47/W and continues to decrease. Therefore, it is possible to drop to USD 0.37/W by 2018. The costs of a solar PV system are composed to that of module, inverter, balance of plant (mounting), engineering, procurement, and commissioning (EPC), human resources and other application fees. Further analyses by ITRI/IEK inChinese Taipei concluded that, during the 2nd quarter of 2016 with module price at USD 0.54/W, the cost breakdown of a solar PV system are as follow: Module accounts for approximately 38.5% of the total costs, inverter accounts for 6%, balance of plant 11%, human resources (including constructions and operation fees) 16%, application

fees for grid connection and selling electricity 0.7%, business communication 0.7%, and other costs (environment impact assessment, structural security, capital deployment) 22.1% and taxes 5%.

6.2 Global trend caused by recent drop in prices of solar power

As mentioned, due to the rapid drop in global demand during the second half of 2016, prices of solar products have dropped drastically. If we look at the prices of solar products in the past five years, the downward trend is significant.
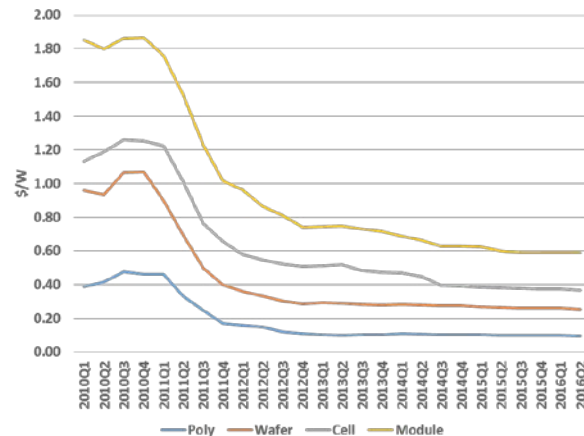

Figure 6.2.1 Global cost trend for wafer, cell and module

As Figure 6.2.1 shows, prices peaked during Q3 of 2010, and dropped all the way until Q4 of 2012. After staying at the same level for two quarters, prices started dropping again in Q3 of 2013. Prices stabilized from Q3 of 2014 to Q2 of 2016. However, prices have dropped by 20% in a Q3 of 2016 alone. We are still observing whether the price drop was caused by inventory reduction.

The price drop has pushed costs of solar power down to a generally acceptable level. Excluding maintenance and interest fees, the cost of solar power has dropped to USD 0.06/kWHr with a 20-year amortization. In comparison, solar power rate in OECD member economies range from USD 0.15 to 0.25/kWHr. For example: Germany USD 0.37/kWHr, Japan USD 0.24/kWHr, UK USD 0.25/kWHr, France USD 0.19/kWHr, US USD 0.13/kWHr. We noticed that voluntary installation has become a trend in many economies.

6.3 Data collection and analysis of solar power policies, comparison between feed-in tariff, subsidized rate and standard rates in major economies

In 2015, the cumulative installation capacity of renewable energy systems (hydraulic power excluded) worldwide is 785GW (Figure6.3.1). Among all energy sources, installation capacity of wind power is the highest while solar power takes second place. Installation capacity in China is the highest, reaching 199GW; United
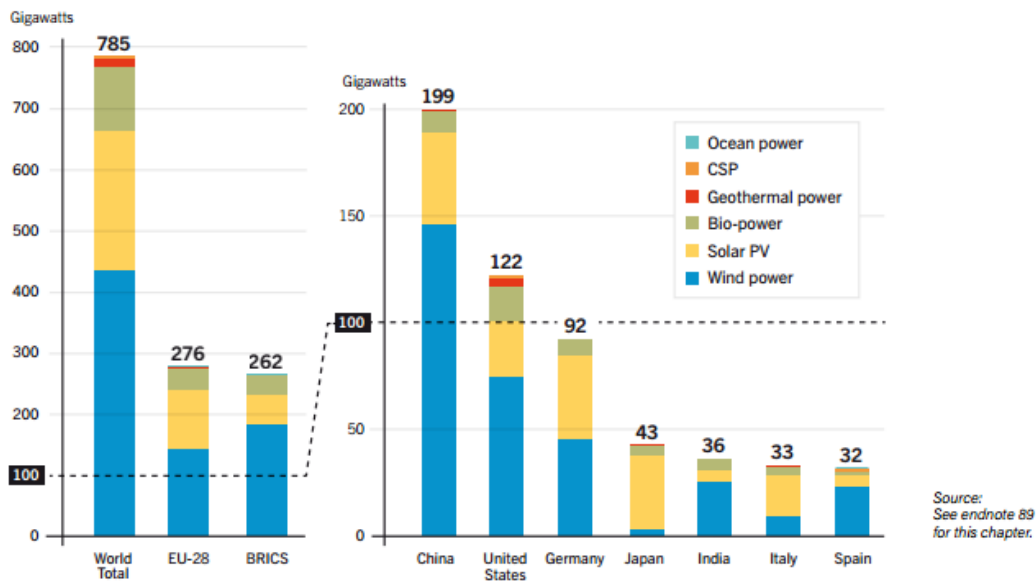
States and Germany came second.

Figure 6.3.1 Cumulative installation capacity of renewable energy systems
(Source: Renewables 2016 Global Status Report)

According to BNEF (Figure 6.3.2), the newly-added installation capacity of 2014 was 45 GW, with an annual growth rate of 12.8%; the additional capacity was 56 GW, while the annual growth rate was 24.4%. It is estimated that the installation capacity will reach 68.9 GW in 2016, with an annual growth rate of 23.0%. This shows that the global solar PV market has experienced double-digits growth in recent years.
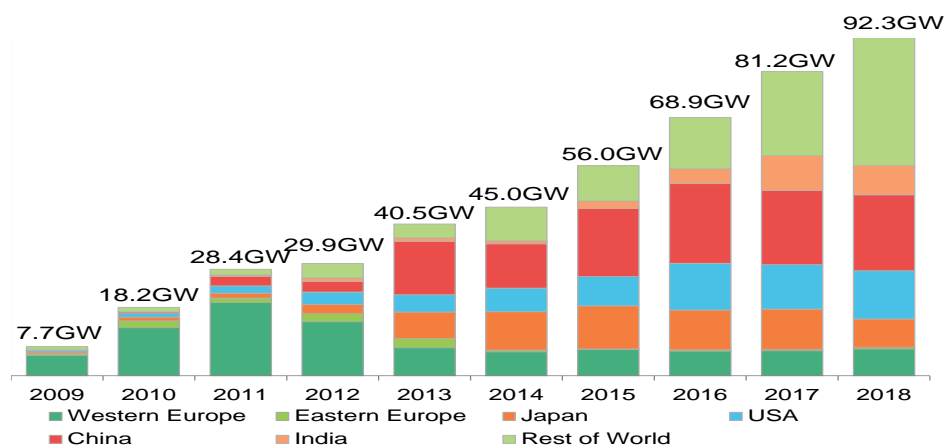

Figure 6.3.2 Global installation capacity forecast from 2009 to 2018

China has become the largest solar PV market worldwide since 2013, and its installation capacity is expected to exceed 20 GW in 2016.

For the past two years, Japan has been the world's second largest market. However, since the Japanese government continues to cut feed-in tariff rates, the installation

capacity of ground-mounted solar power plant has drastically decreased, and the market has been on the decline in 2016. In comparison, the US has a comprehensive, matured financial system. Making use of third-party ownership, installation capacity in the US has been growing steadily—it is estimated to reach 12 GW in 2016, becoming the world's second largest market. Currently, solar PV markets in the US, Australia and Japan are more mature. The reasons are stated below. In the US and Australia, sunlight is abundant. Solar radiation and power generation in certain areas are especially substantial for the markets. Policies in these economies are clear, as well. In Japan, the circumstances are slightly different; due to limited space and high level of urbanization, Japan's electricity demand is high. Consequently, it is suitable for developing distributed residential solar PV systems. Other than the natural advantages, these economies have a long history for developing solar PV industry, the governments have provided comprehensive subsidy and incentive policies, and the companies have developed innovative methods to promote solar PV installation. Aiming to reduce coal, natural gas and nuclear power consumption, governments of Australia, US and Japan have also been devoted to the development and exploitation of renewable energy through making comprehensive policies and establishing adequate mechanisms for industries to flourish. The focus of energy policy in these economies is to turn green energy sources, such as wind, geothermal, and solar power, into the main power sources. Since the solar PV industry in these economies has flourished, we can learn from their experiences. In addition, the emerging major player in the solar PV sector, China, is a case worth looking into as well. By studying these cases, we can provide policy and strategic recommendations for developing the suitable solar PV systems in each economy.

6.3.1 Japan

Japan's market flourished due to two reasons. First, in July 2012, Japanese government published the fixed-rate purchase policy for renewable energy, whose rate is higher and appealing; second, corporations can enjoy tax deduction for investing in renewable power systems of 10 kw and above. The two incentives have successfully driven the development of solar PV market in Japan. In April 2015, the Liberal Democratic Party of Japan proposed a new electricity mix, with nuclear power, coal, hydraulic and geothermal power consisting of 60% of the total electricity mix. The percentage in this proposal is higher than the current 40%, and is even higher than that of before the Fukushima nuclear disaster occurred in March 2011. In particular, nuclear power consists of 20% of the mix; therefore, the proposal has sparked protests by the public in Japan.

As a whole, the Japanese market has encountered drastic cut in FIT prices and newly-

imposed grid connection limitations in 2016 (table 6.3.1.1). However, the installation capacity of plants that are approved for FIT but have not completed constructions is still as high as 55.2 GW. We are following the developments in Japan closely (Figure 6.3.1.1).

Type of Installation	Capacity	2012.7~2013.3	2013.4~2014.3	2014.4~2015.3	2015.4~2015.6	2015.7~2016.3	2016.4~2017.3	Type of Subsidy	Time Period
Residential	<10Kw	42¥/kWh	38¥/kWh	37¥/kWh	See Table below			Excess Power Purchasing	10 years
Non-Residential	>=10Kw	42¥/kWh	37.8¥/kWh	32¥/kWh (pre-tax)	29¥/kWh (pre-tax)	27¥/kWh (pre-tax)	24¥/kWh (pre-tax)	Total Power Purchasing	20 years

Residential <10Kw	2015.4~2016.3		2016.4~2017.3		* Power generated from rooftop solar systems applies to total power purchasing
	Excess Power Purchasing	Combined with Other Types of Energy + Excess Power Purchasing	Excess Power Purchasing	Combined with Other Types of Energy + Excess Power Purchasing	* Since April 1, 2015, PV systems applying for grid connection in regions of Hokkaido, Tohoku, Hokuriku, Chugoku, Shikoku, Kyushu and Okinawa are obliged to install output control equipment.
Output Control Equipment – Installed	35¥/kWh	29¥/kWh	33¥/kWh	27¥/kWh	
Output Control Equipment – Not Installed	33¥/kWh	27¥/kWh	31¥/kWh	25¥/kWh	

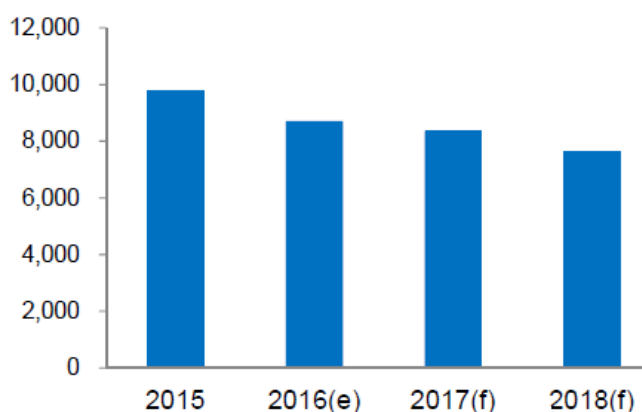**Table 6.3.1.1 The trend of Japan's FIT policy**

Figure 6.3.1.1 Japan's new installation amount (Source: ITRI/IEK)

6.3.2 United States

The US market does not rely on FIT mechanism. Instead, each state in the US specifies the target Renewable Portfolio Standards (RPS) independently. On federal government's front, Investment Tax Credit (ITC) (**Figure 6.3.2.1**) and the Modified Accelerated Cost Recovery System (MACRS) are the most effective policy tools for promoting solar energy. ITC was planned to be decreased since 2017, but was later announced to be extended for 5 more years. ITC remains at 30% until the end of 2019. It will drop to 26% in 2020, 22% in 2021, and will remain at 10% after 2022
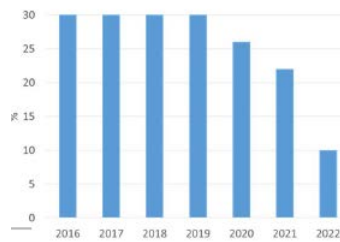
(**Figure 6.3.2.2**).

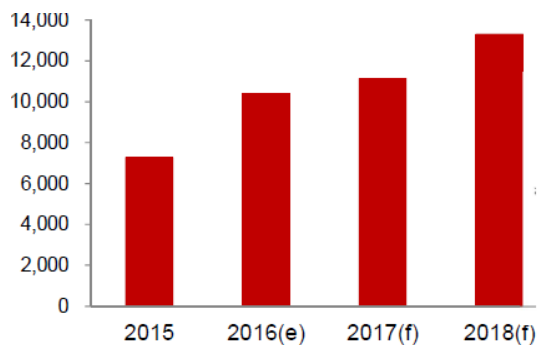**Figure 6.3.2.1 USA ITC plan (Source: DSIRE, 2016, edited by ITRI)**

Figure 6.3.2.2 Additional installation capacity in US (Source: ITRI/IEK)

6.3.3 Australia

In Australia, the carbon tax was abolished in July 2014, and replaced by the Emissions Reduction Fund. The carbon tax has always had mixed reviews. Wholesale electricity in Queensland, Tasmania, South Australia, New South Wales, and Victoria was traded with a FIT mechanism, but will soon be included in the National Electricity Market (NEM); electricity in Northern Territory and Australian Capital Territory has always been traded through NEM. By the end of 2015, the installation capacity of solar PV in Australia reached up to 5GW, concentrating in Queensland, New South Wales, Victoria, South Australia, and Western Australia. The main reason for the current situation is high electricity price. From May 2015 to June 2017, the Australian government presented the "Tony's Tradies" package, targeting small and medium-size enterprises (SME). For SMEs, purchasing solar PV system or battery system can enjoy tax deductions up to AUD 20,000. In September 2015, the Australian Renewable Energy Agency (ARENA) launched a 200 MW large-scale solar auction with a support budget of AUD100 million. The auction was well-received; therefore, ARENA is planning to launch the second auction.

Australia has vast land with low population density, and has abundant traditional and renewable energy resources. After the abolishment of carbon tax and the retirement of

the FIT mechanism, ARENA aims to implement solutions for renewable energy development. In order to increase the use of renewable energy and solar power, ARENA has set up the Emissions Reduction Fund (ERF) with a budget of AUD 2.5 billion. The fund will invest in renewable energy technologies and projects, assisting commercial operations. In addition, because now that states are switching the trade of solar power from FIT mechanism to NEM, market demand will be boosted when operators and electricity companies to set a lower price for solar power.
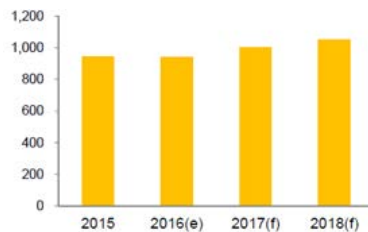

Figure 6.3.3.1 Additional installation capacity in Australia (Source: ITRI/IEK)

6.3.4 China

In China, the policy focus is to expand domestic demand and use limitation of export as leverage in trade talks. China's 13th Five-Year-Plan (135), which aims to add installation capacity by 15 GW to 20 GW from 2016 to 2020, will continue to drive the largest market growth in the world. Since 2016, the benchmark on-grid electricity prices have reduced by CNY 0.1, driving prices down to CNY 0.8 to 0.98/kWHr. Approved applicants of each province's annual capacity management program, the "Front Runner" program of 2015, and the additional 5.3 GW program granted in September 2015 can enjoy the benchmark price of 2015, as long as grid connection is completed before June 30th, 2016. In addition, several cities and provinces have provided additional subsidies with different terms and conditions. By the end of 2015, cumulative installation capacity of solar PV systems in China has reached 43.18 GW. Installation capacity of stationary solar power plants was 37.21 GW, and that of distributed solar power plants reached 6.06 GW, exceeding Germany to become the world's largest market. In 2015, additional installation capacity was 15.13 GW, taking up one-third of the annual output of China's battery module market and providing strong support to the market.
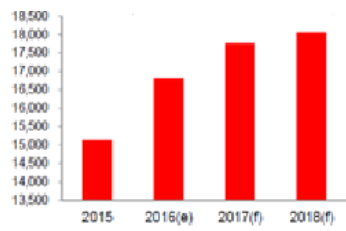
Figure 6.3.4.1 Additional installation capacity in China (Source: ITRI/IEK)

6.4 Collaboration with other APEC economies

H Chemical Co. was established as a separate entity from H Co. in 1962, and committed to develop automobile products, electronic components and energy storage devices and systems. In recent years, economies around the world accelerated economic development, traditional fossil energy sources such as oil, coal, natural gas, etc, were consumed very quickly. It has caused the greenhouse effect and leads to extreme weather and other serious environmental problems. In particular, the 311 earthquake, occurred in Japan in 2011, caused the Fukushima nuclear disaster. People became concerned of the safety of the global nuclear power generation. H Chemical began to be involved in solar cell materials research and development.

In order to improve the competitiveness of silicon solar cells in energy market, solar cell companies continue to reduce production costs of traditional silicon solar cells, they also seek to develop advanced high-efficiency solar cells, such as PERC cells, n-type bifacial solar cells, HIT cells and IBC cells. Compared to conventional single crystalline silicon solar cell manufacturing processes, PERC cell processes simply need to add a back surface passivation and laser opening step, but there is a more than 0.5% increase in cell efficiency. The market share of PERC cells increased gradually recently.

Since the most commonly used material in back surface passivation layer is atomic layer deposition of aluminum oxide, which process is more time-consuming and the equipment is more expensive, H Chemical developed a new passivation paste to be used for the PERC cells back surface passivation layer. It can use conventional screen printing technology to easily produce passivation layer and reduce the production cost of PERC cells.

Compared with conventional p-type solar cells, n-type wafer has better minority carrier lifetime, and has the potential to greatly improve the efficiency of solar cells. Many companies are committed to developing n-type wafer based silicon solar cells, such as n-type bifacial solar cells, HIT cells and IBC cells. But to form the emitter of n-type wafer, it usually needs expensive ion implanter or BBr3 diffusion furnace, which is more difficult to maintain. For this situation, H Chemical developed doping pastes for both p-type wafers and n-type wafers. They can be printed on wafers with traditional screen printing technology, and it only needs a high-temperature furnace to form the emitter. Since the doping area can be easily defined with patterned printing screen, they are more suitable for IBC cell processes or n-type bifacial solar cell selective back surface field process.

ITRI has been involved in the solar cell research and development for a long period,

we have a mature and stable silicon solar cell manufacturing processes, and can provide a good platform to verify the performance of various passivation pastes and doping pastes developed by H Chemical. After some discussion between H Chemical and ITRI, ITRI solar cell group was selected as a partner to assist in the development of passivation pastes for PERC cell and doping pastes for n-type bifacial solar cell and IBC cell. During a 3-year collaboration, H Chemical provided projects of more than NTD 18 million in financial support to ITRI. It also sent two researchers to ITRI to adjust the pastes formula and relevant experimental parameters. After several adjustments in paste formula and process parameters, H Chemical has sent paste samples to domestic solar cell companies to help them in the development of new high-efficiency solar cells.
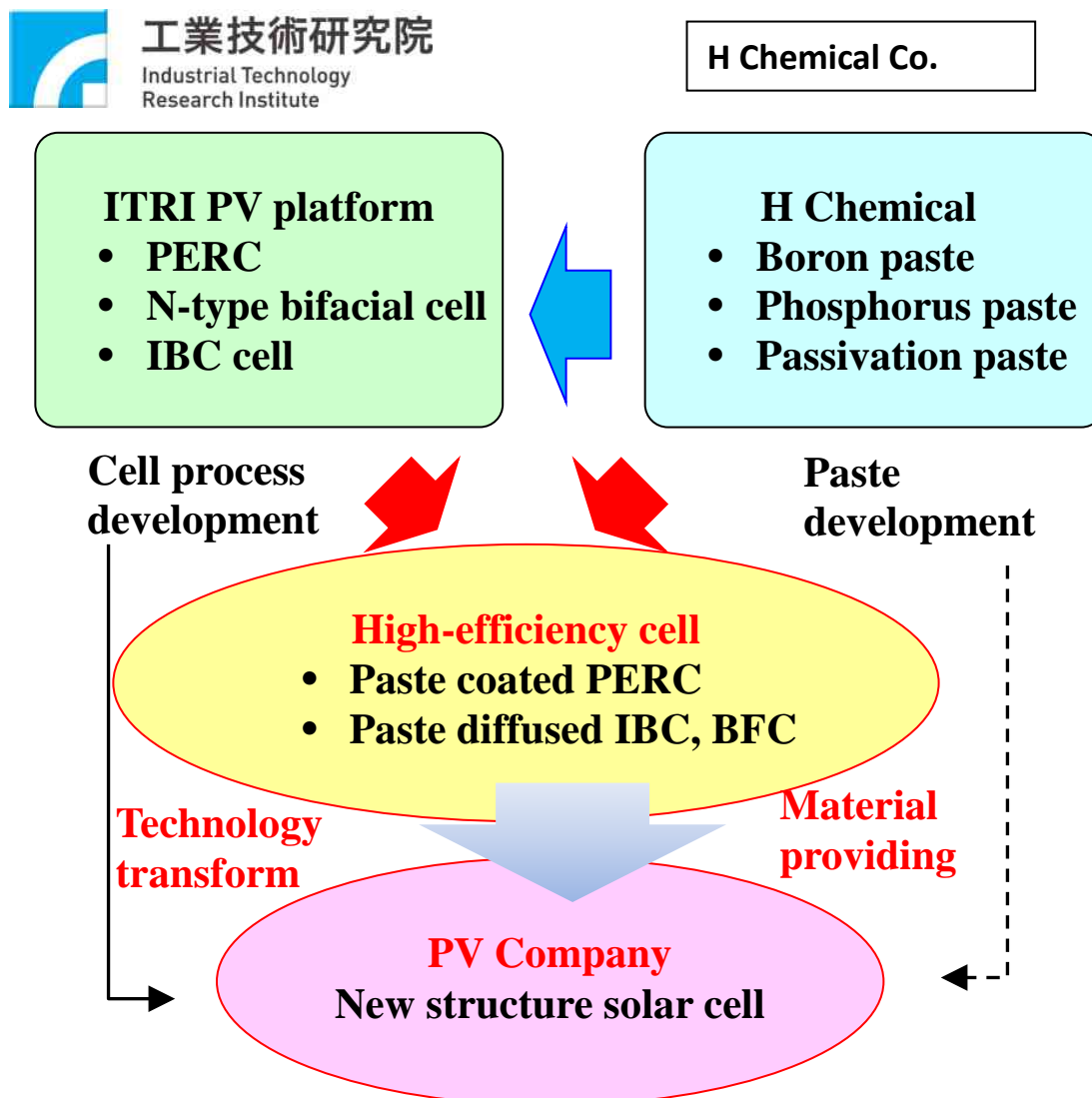

Figure 6.4.1 Collaboration with other APEC economies